positive cell lineage might be cohesive throughout the embryonic cerebral cortical development. By recruiting GFP, we defined the CMWT as the telencephalic region where reelin-positive cell markers are most prominently expressed at the time when most reelin-positive cells are generated, suggesting that this location is a site where prospective reelin-positive cells are generated. Furthermore, at the dorsal and ventral regions of CMWT, the onset of *GFP* expression is followed by those of *reelin* and *p73* differentially, suggesting the existence of heterogeneity of prospective reelin-positive cells that might be distinguished by the differential temporal patterns of reelin-positive cell marker expressions.

Origins of reelin-positive cells in the telencephalon

Our studies on the early expression patterns of reelin-positive cell markers, as with the previous studies, however, do not resolve whether the cells located at putative sources give rise to reelin-positive cells during the cerebral cortical development. By using electroporation-mediated gene transfer (Miyasaka et al., 1999; Saito and Nakatsuji, 2001; Tabata and Nakajima, 2001; Hatanaka and Murakami, 2002), we show here, as expected, prospective reelin-positive cells are generated at the CMWT, including the cortical hem at E11.5. Moreover, it appears the CMWT-derived descendants at the cerebral cortex are solely dedicated to reelin-positive cells. In contrast, the other regions of telencephalon, including the neocortical primordium, where the electroporation was conducted appear to give rise to a few, if any, reelin-positive cells at E11.5. Taking into account of the fact that the prominent expressions of reelin-positive cell markers, including the GFP transgene, are detected focally at the CMWT but not at the other regions of telencephalon, these results indicate that the CMWT is a source for the generation of prospective neocortical reelin-positive cells, among telencephalic regions including neocortical primordium.

A study performed in the *Emx1/2* knock-out mouse (Mallamaci et al., 2000; Shinozaki et al., 2002; Bishop et al., 2003), together with *Emx1*-expressing cell lineage study using *Cre-loxP* system (Gorski et al., 2002), shows that most reelin-positive cells are derived from *Emx1*-expressing progenitors, and *Emx1/2* are required for both reelin-positive cell and subplate generation. On the contrary, a more recent study in the *Sey* mutant mouse was able to show that *Pax6* appear to inhibit reelin-positive cell generation but not, interestingly, subplate generation (Stoykova et al., 2003). Given that *Emx1/2* and *Pax6* expression is in a graded manner in an opposite direction along the rostrolateral–caudomedial axis of the cerebral cortex (O'Leary and Nakagawa, 2002), these studies may imply that the generation of reelin-positive cells are regulated by opposing interactions between *Emx1/2* and *Pax6*. Consistent with this idea, our results indicate that the caudomedially situated *Emx1/2*-high and *Pax6*-low region in the cerebral cortex, namely the CMWT, is spatially allocated for reelin-positive cell generation. Moreover, these mouse genetics studies suggest that the generation of reelin-positive cells and subplate is controlled commonly by *Emx1/2*, but differentially by *Pax6*. This is again consistent with our results showing that the CMWT-derived progenies tangentially migrating into the neocortex are solely dedicated to reelin-positive cells in the MZ, indicating the generation of reelin-positive cell and subplate is differentially controlled.

Tangential migratory behavior and distribution of reelin-positive cells at the neocortex

Our detailed analyses of the electroporated location within the CMWT suggest the cortical hem serves as a source for reelin-positive cells. The cortical hem can be subdivided into two distinct regions in terms of the initial migratory routes of their progenies. In addition, spatial and temporal analyses of expression patterns of *GFP* combined with those of *reelin* and *p73* at the CMWT revealed two distinct subregions within the locus. Taken together, it appears that prospective reelin-positive cells initially expressing *p73* migrate dorsally from the dorsal region of the cortical hem, whereas prospective reelin-positive cells initially expressing *GFP* migrate ventrally from the ventral region of the cortical hem. These studies suggest differential migratory pathways are taken initially depending on the differential subgroups of prospective reelin-positive cells derived from differential origins at the cortical hem.

After exiting the CMWT, the prospective reelin-positive cells invade the neocortical area circumferentially from dorsal, ventral, and posterior directions and set up an overall posterior–anterior cellular influx in the MZ. Our *in vitro* studies support the *in vivo* migratory results and further indicate that the CMWT-derived reelin-positive cells tangentially migrate along the neocortical surface in an overall posterior–anterior direction. Given that apparent uniform localization of reelin-positive cells in the entire cortical MZ, other reelin-positive cell subtypes (*e.g.* subpial granule cells; see Meyer et al., 1998) may tangentially migrate in an opposite anterior–posterior direction. Thus, distinct reelin-positive cell subtypes generated at the distinct locations, including the ones generated at the dorsal and ventral regions of the cortical hem, might tangentially migrate to the cortical MZ in particular directions and comprise the entire population of reelin-positive cells in the cerebral cortex.

We do not know if distinct roles are played by reelin-positive cells derived from the distinct focal locations of the telencephalon in the control of organization of the neocortex. The prospective reelin-positive cells that have been generated at the CMWT at E11.5 cover the posterior half of the neocortex by E13.5, corresponding to the time when the generation of deep layer CP neurons is taking place (Polleux et al., 1997). These tangentially migrating reelin-positive marginal zone cells appear to be continuously supplied and cover the entire neocortical surface in a caudomedial–rostrolateral gradient when a dimension tangential to the surface expands rapidly during the peak period of CP cell generation. Thus, reelin-positive cells extrinsic to the neocortex and CP cells intrinsic to the neocortex appear to intercross with each other at the neocortex and elicit coordinated interactions during the dynamic developmental period of corticogenesis. The spatially and temporally controlled tangential migration of reelin-positive marginal zone cells from the CMWT may therefore underlie the fundamental organization of the neocortex.

One of the most striking scenarios that might be uncovered as a consequence of the present study may concern the way regional or areal specification of the cerebral cortex is established (Grove and Fukuchi-Shimogori, 2003). The issue of areal specification of the neocortex has always raised the question of how cortical areas with enormous dimensions compared with the other regions in the central nervous system would be patterned by the simple diffusion of molecules from the localized signaling centers. Numerous lines of evidence indicate that interactions between the cells with distinct positional identities elicit further specification of the neural characters. The generation and tangential migration of reelin-positive marginal zone cells from one of the putative local signaling centers of the cerebral cortex, the cortical hem, provides an opportunity for the local signaling center to impose positional information onto cells intrinsic to the neocortex. Pertinent to this, the analysis of *Gdf-7* knock-in mice has revealed the existence of tangentially migrating MZ cells in the

Gdf-7-expressing lineage at the CMWT, which may correspond to the tangentially migrating reelin-positive marginal zone cells (Monuki et al., 2001). Whether reelin-positive marginal zone cells that are derived from the CMWT might be involved in the areal as well as laminar organization of developing neocortex awaits further studies.

References

Alcantara S, Ruiz M, D'Arcangelo G, Ezan F, de Lecea L, Curran T, Sotelo C, Soriano E (1998) Regional and cellular patterns of reelin mRNA expression in the forebrain of the developing and adult mouse. J Neurosci 18:7779–7799.

Anderson SA, Eisenstat DD, Shi L, Rubenstein JL (1997) Interneuron migration from basal forebrain to neocortex: dependence on Dlx genes. Science 278:474–476.

Arimatsu Y, Miyamoto M, Nihonmatsu I, Hirata K, Uratani Y, Hatanaka Y, Takiguchi-Hayashi K (1992) Early regional specification for a molecular neuronal phenotype in the rat neocortex. Proc Natl Acad Sci USA 89:8879–8883.

Arimatsu Y, Ishida M, Takiguchi-Hayashi K, Uratani Y (1999) Cerebral cortical specification by early potential restriction of progenitor cells and later phenotype control of postmitotic neurons. Development 126:629–638.

Bishop KM, Garel S, Nakagawa Y, Rubenstein JL, O'Leary DD (2003) Emx1 and Emx2 cooperate to regulate cortical size, lamination, neuronal differentiation, development of cortical efferents, and thalamocortical pathfinding. J Comp Neurol 457:345–360.

Gleeson JG, Walsh CA (2000) Neuronal migration disorders: from genetic diseases to developmental mechanisms. Trends Neurosci 23:352–359.

Gorski JA, Talley T, Qiu M, Puelles L, Rubenstein JL, Jones KR (2002) Cortical excitatory neurons and glia, but not GABAergic neurons, are produced in the Emx1-expressing lineage. J Neurosci 22:6309–6314.

Grove E, Fukuchi-Shimogori T (2003) Generating the cerebral cortical area map. Annu Rev Neurosci 26:355–380.

Grove EA, Tole S, Limon J, Yip L, Ragsdale CW (1998) The hem of the embryonic cerebral cortex is defined by the expression of multiple Wnt genes and is compromised in Gli3-deficient mice. Development 125:2315–2325.

Gupta A, Tsai LH, Wynshaw-Boris A (2002) Life is a journey: a genetic look at neocortical development. Nat Rev Genet 3:342–355.

Hatanaka Y, Murakami F (2002) In vitro analysis of the origin, migratory behavior, and maturation of cortical pyramidal cells. J Comp Neurol 454:1–14.

Hevner RF, Neogi T, Englund C, Daza RA, Fink A (2003) Cajal–Retzius cells in the mouse: transcription factors, neurotransmitters, and birthdays suggest a pallial origin. Brain Res Dev Brain Res 141:39–53.

Imam SA, Young L, Chaiwun B, Taylor CR (1995) Comparison of two microwave based antigen-retrieval solutions in unmasking epitopes in formalin-fixed tissue for immunostaining. Anticancer Res 15:1153–1158.

Ishibashi M, Ang SL, Shiota K, Nakanishi S, Kageyama R, Guillemot F (1995) Targeted disruption of mammalian hairy and Enhancer of split homolog-1 (HES-1) leads to up-regulation of neural helix-loop-helix factors, premature neurogenesis, and severe neural tube defects. Genes Dev 9:3136–3148.

Lavdas AA, Grigoriou M, Pachnis V, Parnavelas JG (1999) The medial ganglionic eminence gives rise to a population of early neurons in the developing cerebral cortex. J Neurosci 19:7881–7888.

Mallamaci A, Mercurio S, Muzio L, Cecchi C, Pardini CL, Gruss P, Boncinelli E (2000) The lack of Emx2 causes impairment of reelin signaling and defects of neuronal migration in the developing cerebral cortex. J Neurosci 20:1109–1118.

Marín-Padilla M (1978) Dual origin of the mammalian neocortex and evolution of the cortical plate. Anat Embryol (Berl) 152:109–126.

Marín-Padilla M (1998) Cajal–Retzius cells and the development of the neocortex. Trends Neurosci 21:64–71.

Meyer G, Soria JM, Martinez-Galan JR, Martin-Clemente B, Fairen A (1998) Different origins and developmental histories of transient neurons in the marginal zone of the fetal and neonatal rat cortex. J Comp Neurol 397:493–518.

Meyer G, Goffinet AM, Fairen A (1999) What is a Cajal–Retzius cell? A reassessment of a classical cell type based on recent observations in the developing neocortex. Cereb Cortex 9:765–775.

Meyer G, Schaaps JP, Moreau L, Goffinet AM (2000) Embryonic and early fetal development of the human neocortex. J Neurosci 20:1858–1868.

Meyer G, Perez-Garcia CG, Abraham H, Caput D (2002) Expression of p73 and reelin in the developing human cortex. J Neurosci 22:4973–4986.

Miyasaka N, Arimatsu Y, Takiguchihayashi K (1999) Foreign gene expression in an organotypic culture of cortical anlage after in vivo electroporation. NeuroReport 10:2319–2323.

Monuki ES, Porter FD, Walsh CA (2001) Patterning of the dorsal telencephalon and cerebral cortex by a roof plate-Lhx2 pathway. Neuron 32:591–604.

Motoyama J, Kitajima K, Kojima M, Kondo S, Takeuchi T (1997) Organogenesis of the liver, thymus and spleen is affected in jumonji mutant mice. Mech Dev 66:27–37.

Muneoka K, Wanek N, Bryant SV (1986a) Mouse embryos develop normally exo utero. J Exp Zool 239:289–293.

Muneoka K, Wanek N, Bryant SV (1986b) Exo utero survival of mouse embryos. Prog Clin Biol Res 217A:305–308.

Nadarajah B, Parnavelas JG (2002) Modes of neuronal migration in the developing cerebral cortex. Nat Rev Neurosci 3:423–432.

Ngo-Muller V, Muneoka K (2000) Exo utero surgery. Methods Mol Biol 135:481–492.

Ogawa M, Miyata T, Nakajima K, Yagyu K, Seike M, Ikenaka K, Yamamoto H, Mikoshiba K (1995) The reeler gene-associated antigen on Cajal–Retzius neurons is a crucial molecule for laminar organization of cortical neurons. Neuron 14:899–912.

O'Leary DD, Nakagawa Y (2002) Patterning centers, regulatory genes and extrinsic mechanisms controlling arealization of the neocortex. Curr Opin Neurobiol 12:14–25.

Polleux F, Dehay C, Kennedy H (1997) The timetable of laminar neurogenesis contributes to the specification of cortical areas in mouse isocortex. J Comp Neurol 385:95–116.

Rice DS, Curran T (2001) Role of the reelin signaling pathway in central nervous system development. Annu Rev Neurosci 24:1005–1039.

Saito T, Nakatsuji N (2001) Efficient gene transfer into the embryonic mouse brain using in vivo electroporation. Dev Biol 240:237–246.

Schaeren-Wiemers N, Gerfin-Moser A (1993) A single protocol to detect transcripts of various types and expression levels in neural tissue and cultured cells: in situ hybridization using digoxigenin-labelled cRNA probes. Histochemistry 100:431–440.

Schiffmann SN, Bernier B, Goffinet AM (1997) reelin mRNA expression during mouse brain development. Eur J Neurosci 9:1055–1071.

Shinozaki K, Miyagi T, Yoshida M, Miyata T, Ogawa M, Aizawa S, Suda Y (2002) Absence of Cajal–Retzius cells and subplate neurons associated with defects of tangential cell migration from ganglionic eminence in Emx1/2 double mutant cerebral cortex. Development 129:3479–3492.

Soda T, Nakashima R, Watanabe D, Nakajima K, Pastan I, Nakanishi S (2003) Segregation and coactivation of developing neocortical layer 1 neurons. J Neurosci 23:6272–6279.

Stoykova A, Hatano O, Gruss P, Gotz M (2003) Increase in reelin-positive cells in the marginal zone of Pax6 mutant mouse cortex. Cereb Cortex 13:560–571.

Supèr H, Soriano E, Uylings HB (1998) The functions of the preplate in development and evolution of the neocortex and hippocampus. Brain Res Brain Res Rev 27:40–64.

Tabata H, Nakajima K (2001) Efficient in utero gene transfer system to the developing mouse brain using electroporation: visualization of neuronal migration in the developing cortex. Neuroscience 103:865–872.

Takiguchi-Hayashi K, Sato M, Sugo N, Ishida M, Sato K, Uratani Y, Arimatsu Y (1998) Latexin expression in smaller diameter primary sensory neurons in the rat. Brain Res 801:9–20.

Tissir F, Goffinet AM (2003) reelin and brain development. Nat Rev Neurosci 4:496–505.

Watanabe D, Inokawa H, Hashimoto K, Suzuki N, Kano M, Shigemoto R, Hirano T, Toyama K, Kaneko S, Yokoi M, Moriyoshi K, Suzuki M, Kobayashi K, Nagatsu T, Kreitman RJ, Pastan I, Nakanishi S (1998) Ablation of cerebellar Golgi cells disrupts synaptic integration involving GABA inhibition and NMDA receptor activation in motor coordination. Cell 95:17–27.

Wood JG, Martin S, Price DJ (1992) Evidence that the earliest generated cells of the murine cerebral cortex form a transient population in the subplate and marginal zone. Brain Res Dev Brain Res 66: 137–140.

Available online at www.sciencedirect.com
SCIENCE DIRECT®
ELSEVIER
Biochemical and Biophysical Research Communications 324 (2004) 1319–1323
BBRC
www.elsevier.com/locate/ybbrc

Cardiac abnormalities cause early lethality of *jumonji* mutant mice

Miho Takahashi[a,b], Mizuyo Kojima[a], Kuniko Nakajima[a], Rika Suzuki-Migishima[a], Yoshiko Motegi[a], Minesuke Yokoyama[a,1], Takashi Takeuchi[a,b,*]

[a] *Mitsubishi Kagaku Institute of Life Sciences (MITILS), 11 Minamiooya, Machida, Tokyo 194-8511, Japan*
[b] *Graduate School of Environment and Information Sciences, Yokohama National University, 79-1 Tokiwadai, Hodogaya, Yokohama 240-8501, Japan*

Received 21 September 2004
Available online 12 October 2004

Abstract

jumonji (*jmj*) mutant mice, obtained by a gene trap strategy, showed several morphological abnormalities including neural tube and cardiac defects, and died in utero around embryonic day 11.5 (E11.5). It is unknown what causes the embryonic lethality. Here, we demonstrate that exogenous expression of *jmj* gene in the heart of *jmj* mutant mice rescued the morphological phenotypes in the heart, and these embryos survived until E13.5. These results suggest that there are at least two lethal periods in *jmj* mutant mice, and that cardiac abnormalities may cause the earlier lethality. In addition, the rescue of the cardiac abnormalities by the *jmj* transgene provided solid evidence that the cardiac abnormalities resulted from mutation of the *jmj* gene.

Keywords: jumonji; Transcriptional repressor; Cardiac morphogenesis; Cardiac myocyte; Embryonic lethality; Gene trap; Transgenic mouse; Mutant mouse

Embryonic lethality is one of major phenotypes in mutant animals and the embryos die of various defects, for example, hematopoietic or cardiac defects.

jumonji (*jmj*) homozygous mice, originally obtained by a mouse gene trap strategy, show embryonic lethality [1]. These mice also exhibit various abnormalities such as neural tube, cardiac and hematopoietic defects [1–6]. These phenotypes are dependent largely on the mouse genetic backgrounds. Mutant mice with a C3H/He background exhibit neural tube defects, abnormal morphology of the right ventricle, and hyperproliferation of trabecular cardiac myocytes, and die around E11.5 [3]. Our recent studies on hyperproliferation of trabecular cardiac myocytes showed that this abnormality resulted from enhanced expression of cyclin D1 [7], which is one of the key components of the cell cycle machinery. On the other hand, mutant mice with a BALB/c background exhibit hematopoietic defects but not neural tube defects or hyperproliferation of trabecular cardiac myocytes, and die around E15.5 [2,4,6].

Molecular analysis has indicated that trap vectors were introduced into one intron of the gene designated as *jmj* and disrupted the function of this gene [1,8]. The *jmj* gene encodes a protein that is a member of the jumonji family [9] and the AT-rich interaction domain (ARID) family [10]. The ARID is a DNA-binding domain and several members of this family are known to be transcriptional factors and are involved in a variety of biological processes [10]. Recently, we and Kim et al. showed that Jmj protein is a transcriptional repressor [7,11]. We also showed that Jmj downregulates cardiac myocyte proliferation by repressing *cyclin D1* transcription [7].

Despite these results, the reasons for the embryonic lethality are still unknown. In the case of mutant mice with a C3H/He background, embryos are likely to die

* Corresponding author. Fax: +81 42 724 6267.
E-mail address: take@libra.ls.m-kagaku.co.jp (T. Takeuchi).
[1] Present address. Department of Comparative and Experimental Medicine, Niigata Brain Research Institute, 1-757 Asahi-machi-dori Niigata, Niigata, 951-8585 Japan.

0006-291X/$ - see front matter © 2004 Elsevier Inc. All rights reserved.
doi:10.1016/j.bbrc.2004.09.203

of cardiac abnormalities, but we could not exclude the possibility that mutant mice die of other known or unknown phenotypes. Therefore, we tried to rescue cardiac abnormalities by exogenous expression of *jmj* in the heart and analyzed the lethality.

Materials and methods

Mice. CAJ17 transgenic mice with a C3H/He background carrying the pCAJIE vector were produced as described previously [7]. *jmj* heterozygous mice carrying a *CAJ17* transgene ($jmj^{trap/+}$/*CAJ17*(+)) were obtained by crossing *CAJ17* hemizygous mice with F18-25 $jmj^{trap/+}$ mice with a C3H/He background. $jmj^{trap/+}$/*CAJ17*(+) mice were mated with $jmj^{trap/+}$ mice to produce *jmj* homozygous mice carrying a *CAJ17* transgene ($jmj^{trap/trap}$/*CAJ17*(+)), and we compared the phenotypes with those of $jmj^{trap/trap}$ littermates not carrying a *CAJ17* transgene ($jmj^{trap/trap}$/*CAJ17*(−)). Mice were genotyped by PCR as described previously [1] for the *jmj* allele. *CAJ17*(+) mice were identified by PCR using primers 5′-GTGAACTGCCACATGACAGT-3′ and 5′-CAGCAGGTTGAACCCAAAGT-3′. PCR was carried out by denaturing the DNA at 94 °C for 1 min, followed by 35 cycles at 94 °C for 1 min, 60 °C for 1 min, 72 °C for 2 min, and a final extension step at 72 °C for 8 min.

The presence of a vaginal plug was regarded as E0.5. Embryos with a beating heart or existence of blood flow in the umbilical cord were considered to be live embryos.

Histology. Embryos were dissected in Dulbecco's phosphate-buffered saline (PBS) and fixed overnight at 4 °C in Bouin's fixative (Sigma Diagnostics, St. Louis, MO) for hematoxylin and eosin (HE) staining.

Cells which showed chromosomes but neither nuclear membrane nor nucleolus were counted as mitotic cells in sections stained with HE and the (number of mitotic cells/number of total cells) × 100 was presented as the mitotic index. More than 1400 cells per embryo were examined as total cells in the trabecular layer at E10.5.

Statistical analysis. The experimental data were analyzed using Fisher' exact test. In addition, we used Fisher's least significant difference (LSD) test after obtaining a significant difference with one-way analysis of variance (ANOVA) for multiple comparison tests. Values of $P < 0.05$ were considered as statistically significant.

Results

The jmj transgene rescued the morphological abnormalities in the heart of jmj mutant embryos

We have established a transgenic mouse line, *CAJ17* [7]. The expression pattern of the exogenous *jmj* gene can be monitored by green fluorescent protein (GFP) because GFP is co-expressed with Jmj proteins via an internal ribosome entry site [7]. *CAJ17* mice at E10.5 exhibited strong expression of GFP in the heart (Fig. 1, arrow) where abnormal morphologies are observed in *jmj* mutant embryos [3], and weaker expression in small regions around the neural tube where no abnormalities are revealed in the mutant embryos (data not shown). The *jmj* mRNA level in the cardiac ventricles of transgenic embryos (*CAJ17*(+)) increased approximately four times compared to non-transgenic embryos

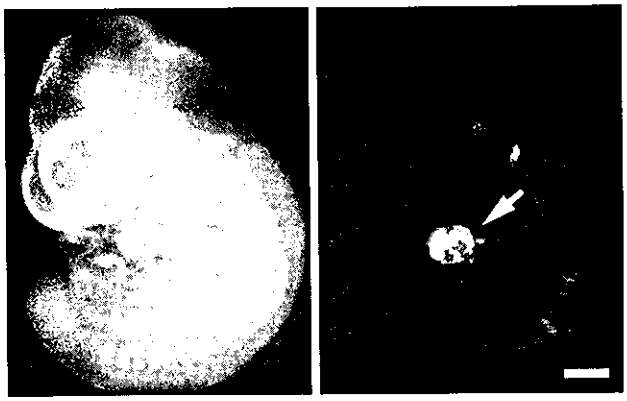

Fig. 1. Expression pattern of the transgene in *CAJ17*(+) embryos at E10.5. Left panel, bright fields; right panel, dark fields for GFP observation. GFP is strongly expressed in the heart (arrow). Scale bar, 500 μm.

(*CAJ17*(−)) [7]. The expression pattern in the heart continued to adulthood. Hemizygous mice of the line showed no apparent abnormalities. We examined whether the cardiac abnormalities of *jmj* mutant embryos could be rescued using this mouse line.

jmj homozygous ($jmj^{trap/trap}$) embryos with a C3H/HeJ background exhibit abnormal morphology in the right ventricle and hyperplasia of trabecular cardiac myocytes at E10.5-11.5 [3] (Fig. 2). We introduced the exogenous *jmj* gene into $jmj^{trap/trap}$ embryos by crossing, and compared the phenotypes of $jmj^{trap/trap}$ embryos carrying the *CAJ17* transgene ($jmj^{trap/trap}$/*CAJ17*(+)) with those of $jmj^{trap/trap}$ littermates not carrying the *CAJ17*

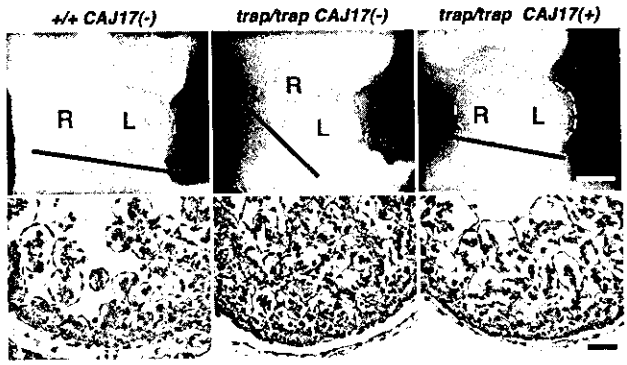

Fig. 2. Exogenous expression of *jmj* gene rescues abnormal morphologies of the heart of *jmj* mutant mice. Cardiac morphology of a representative embryo of wild type (+/+*CAJ17*(−)), $jmj^{trap/trap}$/*CAJ17*(−) (*trap/trap CAJ17*(−)), and $jmj^{trap/trap}$/*CAJ17*(+) (*trap/trap CAJ17*(+)) embryos at E11.5. Upper and bottom panels show front views of the heart after fixation with Bouin's solution, and sections of the left ventricles stained with HE, respectively. White and black scale bars, 300 and 50 μm, respectively. Black lines, white dot lines, L and R in upper panels show the position of the caudal base of the ventricles, outlines of the hearts, and the left and right ventricles, respectively. Note that the abnormal position of the right ventricle (upper panel) and abnormal morphology (hyperplasia) of trabeculae (bottom panel) of the *jmj* mutant embryo were rescued by *CAJ17* transgenes.

transgene ($jmj^{trap/trap}/CAJ17(-)$) at E11.5 in order to examine the effects of exogenous expression of *jmj* gene in the heart on these phenotypes.

The ratio of embryos with abnormal morphology of the right ventricle largely decreased in $jmj^{trap/trap}/CAJ17(+)$ embryos (28.6%, $N = 7$), compared to that in $jmj^{trap/trap}/CAJ17(-)$ embryos (100%, $N = 6$) (Fig. 2, upper panels). Trabeculae in the ventricles of all $jmj^{trap/trap}/CAJ17(-)$ embryos ($N = 4$) revealed a disordered structure and often showed degenerative morphology, while those in all $jmj^{trap/trap}/CAJ17(+)$ embryos examined ($N = 4$) showed a normal projecting structure similar to that of wild type embryos (Fig. 2, bottom panels). Fisher's exact test demonstrated that the difference between $jmj^{trap/trap}/CAJ17(+)$ and $jmj^{trap/trap}/CAJ17(-)$ embryos was significant (abnormal morphology of the right ventricle, $P = 0.016$; abnormal morphology of trabeculae, $P = 0.014$).

Abnormal morphology of trabeculae resulted from hyperproliferation of trabecular cardiac myocytes in $jmj^{trap/trap}$ embryos [3,7]. The mitotic index (MI) of trabecular myocytes in the cardiac ventricles of $jmj^{trap/trap}$ embryos increased [3] (Fig. 3). Therefore, we examined whether exogenous *jmj* expression can rescue this phenotype. The mean of MI of $jmj^{trap/trap}/CAJ17(+)$ embryos was between those of $jmj^{trap/trap}/CAJ17(-)$ and normal embryos ($jmj^{+/+}/CAJ17(-)$ and $jmj^{trap/+}/CAJ17(-)$) (Fig. 3). Fisher's LSD test indicated that MI of $jmj^{trap/trap}/CAJ17(+)$ embryos were significantly lower than those of $jmj^{trap/trap}/CAJ17(-)$ ($P = 0.031$), after obtaining a significant difference with one-way ANOVA ($F_{(2,6)} = 14.39$, $P = 0.0051$).

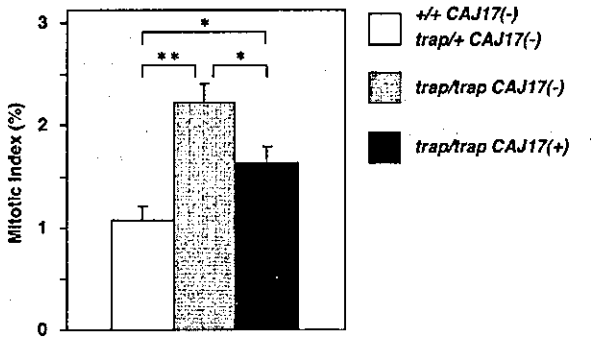

Fig. 3. Exogenous expression of *jmj* gene rescues enhanced proliferation of cardiac myocytes of *jmj* mutant mice. MI of trabecular myocytes of left ventricles in wild type and *jmj* heterozygous (+/+ *CAJ17*(−) and *trap*/+ *CAJ17*(−)), $jmj^{trap/trap}/CAJ17(-)$ (*trap*/*trap* *CAJ17*(−)), and $jmj^{trap/trap}/CAJ17(+)$ (*trap*/*trap* *CAJ17*(+)) embryos at E11.5. MI are presented as means ± standard error of three embryos. * and ** are $P < 0.05$ and 0.005, respectively (Fisher's LSD test after one-way ANOVA).

These results show that the exogenous *jmj* gene can rescue cardiac phenotypes of $jmj^{trap/trap}$ embryos.

Early lethality of jmj mutant mice was rescued by the jmj transgene

Embryonic lethality was one of the main phenotypes of $jmj^{trap/trap}$ embryos. $jmj^{trap/trap}$ embryos with a C3H/He background die around E11.5 [3]. We examined whether the lethality could be rescued by the *jmj* transgene. *jmj* heterozygous and *CAJ17* hemizygous mice ($jmj^{trap/+}/CAJ17(+)$) were mated with *jmj* heterozygous mice ($jmj^{trap/+}/CAJ17(-)$), and embryos were genotyped in various embryonic stages. The numbers of live (with beating hearts) and dead $jmj^{trap/trap}$ embryos (without beating hearts) were then examined (Table 1).

While all $jmj^{trap/trap}$ embryos were alive irrespective of the existence of a *CAJ17* transgene at E8.5, half and all $jmj^{trap/trap}/CAJ17(-)$ embryos were dead at E11.5 and E13.5, respectively. On the other hand, all $jmj^{trap/trap}/CAJ17(+)$ embryos were alive as far as these stages. Fisher's exact test showed that the differences between $jmj^{trap/trap}/CAJ17(+)$ and $jmj^{trap/trap}/CAJ17(-)$ embryos were significant (E11.5, $P = 0.034$; E13.5, $P = 0.003$). The appearance of $jmj^{trap/trap}/CAJ17(+)$ embryos at E13.5 was similar to $jmj^{trap/trap}$ embryos with a BALB/c background at the same stage [2,4] (Fig. 4). These embryos were pale and their livers were also pale and small (Fig. 4, arrow). No $jmj^{trap/trap}$ embryos, irrespective of the existence of a *CAJ17* transgene, were obtained after E15.5.

Table 1
Number of live and dead $jmj^{trap/trap}$ embryos carrying or not carrying *CAJ17* transgene

Embryonic day	$jmj^{trap/trap}/CAJ17(-)$			$jmj^{trap/trap}/CAJ17(+)$		
	Live	Dead	Total (live %)	Live	Dead	Total (live %)
8.5	5	0	5 (100)	7	0	7 (100)
11.5	6	6	12 (50)	7	0	7 (100)*
13.5	0	4	4 (0)	7	0	7 (100)**
15.5	0	1	1 (0)	0	3	3 (0)
Total	8	11	19 (42.1)	21	3	24 (87.5)**

Numbers of embryos which could be genotyped are shown. Numbers in parentheses show percentages of live embryos among total embryos. (*,**) The ratios of the live $jmj^{trap/trap}$ *CAJ17*(+) embryos were significantly higher than those of $jmj^{trap/trap}$ *CAJ17*(−) embryos. *$P < 0.05$; **$P < 0.005$, Fisher's exact tests.

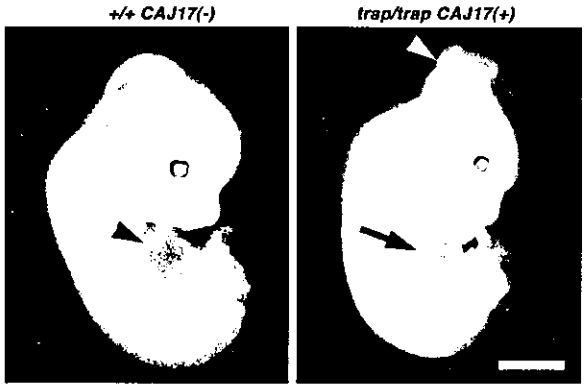

Fig. 4. Morphology of *jmj* mutant embryos which survived until E13.5. Whole mount views of wild type (+/+ *CAJ17*(−)) and *jmj*$^{trap/trap}$/*CAJ17*(+) (*trap/trap CAJ17*(+)) embryos at E13.5. The black arrowhead and arrow indicate a normal liver in a wild type embryo, and small and pale livers in *jmj*$^{trap/trap}$/*CAJ17*(+) embryos, respectively. *jmj*$^{trap/trap}$/*CAJ17*(+) embryo shows neural tube defects (white arrowhead). Scale bar, 2 mm.

These results demonstrate that the *jmj* transgenes could rescue the earlier lethality of *jmj* mutant mice.

Discussion

In this paper, we examined whether the lethality of *jmj* mutant embryos around E11.5 resulted from the cardiac abnormalities. Our data showed that exogenous expression of *jmj* in the heart rescued the cardiac abnormalities significantly. These embryos survived up to E13.5. These results suggest that the lethality of *jmj* mutant embryos around E11.5 resulted from the cardiac abnormalities.

What is the cause of the lethality? Two cardiac abnormalities, abnormal morphology in the right ventricle and hyperplasia of trabecular cardiac myocytes, have been observed. Abnormal morphology in the right ventricle can be excluded as a cause of the lethality because *jmj* and *cyclin D1* double mutant mice exhibited this abnormality [7] but can survive up to E13.5 (Takahashi et al., unpublished data). Since hyperplasia of trabecular cardiac myocytes was rescued in the double mutant mice [7] and *jmj* mutant embryos appear not to maintain sufficient cardiac output by this abnormality, hyperplasia of trabecular cardiac myocytes would appear to be the cause of the lethality.

The exogenous *jmj* expression demonstrates an ability to rescue the lethality until E13.5 but not after E15.5. This fact suggests that there are at least two lethal stages (early and late) in *jmj*$^{trap/trap}$ embryos with a C3H/He background and the exogenous *jmj* expression can rescue only early lethality.

Interestingly, *jmj*$^{trap/trap}$ embryos with a BALB/c background died around E15.5, probably of anemia [4], and the appearance of embryos at E13.5-14.5 is very similar to that of *jmj*$^{trap/trap}$/*CAJ17*(+) embryos shown here [2,4]. The livers of both *jmj*$^{trap/trap}$ embryos with a BALB/c background and *jmj*$^{trap/trap}$/*CAJ17*(+) embryos were pale and small. These facts suggest that the cause of late lethality in *jmj*$^{trap/trap}$ embryos with a C3H/He background is the same as those with a BALB/c background, and that exogenous *jmj* expression in the heart could not rescue the phenotype.

It was necessary to examine whether the *jmj* gene is responsible for the phenotypes of *jmj* mutant mice. Although previous studies suggest that mutation of the *jmj* gene causes the phenotypes, we could not exclude the possibility that the phenotypes result from mutation(s) in the other gene(s) neighboring or within the *jmj* gene or in both these genes and the *jmj* gene. It is possible that insertion of the trap vector could affect the function of genes within the *jmj* gene because some genes, whose EST clones were reported and their functions are unknown, are found in the 1st intron of the mouse *jmj* gene in which the trap vector is inserted. The results described in this paper have shown clearly that the *jmj* gene is responsible for at least the cardiac phenotypes of *jmj* mutant mice.

Because cardiac defects are one of the most frequent causes of embryonic lethality, our results are very important for understanding the mechanisms of embryonic lethality as well as the mechanisms regulating cardiac development.

Acknowledgment

This work was partially supported by a research grant from the Ministry of Education, Culture, Sports, Science and Technology of Japan.

References

[1] T. Takeuchi, Y. Yamazaki, Y. Katoh-Fukui, R. Tsuchiya, S. Kondo, J. Motoyama, T. Higashinakagawa, Gene trap capture of a novel mouse gene, jumonji, required for neural tube formation, Genes Dev. 9 (1995) 1211–1222.
[2] J. Motoyama, K. Kitajima, M. Kojima, S. Kondo, T. Takeuchi, Organogenesis of the liver, thymus and spleen is affected in jumonji mutant mice, Mech. Dev. 66 (1997) 27–37.
[3] T. Takeuchi, M. Kojima, K. Nakajima, S. Kondo, jumonji gene is essential for the neurulation and cardiac development of mouse embryos with a C3H/He background, Mech. Dev. 86 (1999) 29–38.
[4] K. Kitajima, M. Kojima, K. Nakajima, S. Kondo, T. Hara, A. Miyajima, T. Takeuchi, Definitive but not primitive hematopoiesis is impaired in jumonji mutant mice, Blood 93 (1999) 87–95.
[5] Y. Lee, A.J. Song, R. Baker, B. Micales, S.J. Conway, G.E. Lyons, Jumonji, a nuclear protein that is necessary for normal heart development, Circ. Res. 86 (2000) 932–938.
[6] K. Kitajima, M. Kojima, S. Kondo, T. Takeuchi, A role of jumonji gene in proliferation but not differentiation of megakaryocyte lineage cells, Exp. Hematol. 29 (2001) 507–514.

[7] M. Toyoda, H. Shirato, K. Nakajima, M. Kojima, M. Takahashi, M. Kubota, R. Suzuki-Migishima, Y. Motegi, M. Yokoyama, T. Takeuchi, jumonji downregulates cardiac cell proliferation by repressing cyclin D1 expression., Dev. Cell 5 (2003) 85–97.
[8] M. Toyoda, M. Kojima, T. Takeuchi, Jumonji is a nuclear protein that participates in the negative regulation of cell growth, Biochem. Biophys. Res. Commun. 274 (2000) 332–336.
[9] D. Balciunas, H. Ronne, Evidence of domain swapping within the jumonji family of transcription factors, Trends Biochem. Sci. 25 (2000) 274–276.
[10] R.D. Kortschak, P.W. Tucker, R. Saint, ARID proteins come in from the desert, Trends Biochem. Sci. 25 (2000) 294–299.
[11] T.G. Kim, J.C. Kraus, J. Chen, Y. Lee, JUMONJI, a critical factor for cardiac development, functions as a transcriptional repressor, J. Biol. Chem. 278 (2003) 42247–42255.

Regulation of oxidative stress by ATM is required for self-renewal of haematopoietic stem cells

Keisuke Ito[1,2*], Atsushi Hirao[1*], Fumio Arai[1], Sahoko Matsuoka[1], Keiyo Takubo[1], Isao Hamaguchi[1], Kana Nomiyama[1], Kentaro Hosokawa[1], Kazuhiro Sakurada[3], Naomi Nakagata[4], Yasuo Ikeda[2], Tak W. Mak[5] & Toshio Suda[1]

[1]*Department of Cell Differentiation, The Sakaguchi Laboratory of Developmental Biology, Keio University School of Medicine, 35 Shinano-machi, Shinjuku-ku, Tokyo 160-8582, Japan*
[2]*Division of Hematology, Department of Internal Medicine, Keio University School of Medicine, 35 Shinano-machi, Shinjuku-ku, Tokyo 160-8582, Japan*
[3]*BioFrontier Laboratories, Kyowa Hakko Kogyo Co. Ltd, Machida-shi, Tokyo 194-8533, Japan*
[4]*Division of Reproductive Engineering, Center for Animal Resources and Development, Kumamoto University, Honjo, Kumamoto 860-0811 Japan*
[5]*Advanced Medical Discovery Institute, Ontario Cancer Institute, Departments of Medical Biophysics and Immunology, University of Toronto, 620 University Avenue, Suite 706, Toronto, Ontario M5G 2C1, Canada*

*These authors contributed equally to this work

The 'ataxia telangiectasia mutated' (*Atm*) gene maintains genomic stability by activating a key cell-cycle checkpoint in response to DNA damage, telomeric instability or oxidative stress[1,2]. Mutational inactivation of the gene causes an autosomal recessive disorder, ataxia–telangiectasia, characterized by immunodeficiency, progressive cerebellar ataxia, oculocutaneous telangiectasia, defective spermatogenesis, premature ageing and a high incidence of lymphoma[3,4]. Here we show that ATM has an essential function in the reconstitutive capacity of haematopoietic stem cells (HSCs) but is not as important for the proliferation or differentiation of progenitors, in a telomere-independent manner. *Atm*$^{-/-}$ mice older than 24 weeks showed progressive bone marrow failure resulting from a defect in HSC function that was associated with elevated reactive oxygen species. Treatment with anti-oxidative agents restored the reconstitutive capacity of *Atm*$^{-/-}$ HSCs, resulting in the prevention of bone marrow failure. Activation of the p16^{INK4a}-retinoblastoma (Rb) gene product pathway in response to elevated reactive oxygen species led to the failure of *Atm*$^{-/-}$ HSCs. These results show that the self-renewal capacity of HSCs depends on ATM-mediated inhibition of oxidative stress.

It has been shown that many factors are crucial in determining the fate of stem cells, yet molecular mechanisms governing the maintenance of the self-renewal capacity have not been well studied. Wong *et al.*[5] recently reported an interesting linkage between ATM and stem cell function. This group demonstrated that *Atm* deficiency, in combination with telomerase RNA component (Terc) deficiency, led to neural stem cell failure characterized by increased telomere erosion. In contrast, *Atm* deficiency alone did not affect neural stem cells. To investigate roles of ATM on self-renewal of stem cells in detail, we evaluated the effects of *Atm* deficiency on the haematopoietic system in this study.

Other than the previously reported defect in T cell development[6–9], *Atm*$^{-/-}$ mice showed normal numbers and subsets of haematopoietic cells in peripheral blood at 8 weeks of age. The loss of ATM did not show any defect in the differentiation or proliferation potential of progenitors at this age (Supplementary Fig. 1). The percentages of S/G2/M phases of the cell cycle in c-Kit$^+$Sca-1$^+$Lineage$^-$ (KSL) cells were equal in wild-type (WT; 12.15 ± 1.60%) and *Atm*$^{-/-}$ mice (13.36 ± 2.81%). Next we investigated whether more primitive haematopoietic cells, HSCs, are affected in *Atm*$^{-/-}$ bone marrow (BM). The frequencies of the stem cell subsets CD34$^{-/low}$KSL, Thy1^{low}KSL and Tie2$^+$KSL (as defined by cell surface markers[10–12]) were significantly reduced in *Atm*$^{-/-}$ BM (Fig. 1a). The number of colony-forming cells derived from *Atm*$^{-/-}$ KSL cells after 6 weeks of culture on stromal cells was significantly decreased compared with that of the WT, although a short-term culture (less than 2 weeks) did not show a significant difference (Fig. 1b). To assess the repopulating ability of *Atm*$^{-/-}$ HSCs directly *in vivo*, we performed a competitive reconstitution assay in which BM mononuclear cells (MNCs) from *Atm*$^{-/-}$ mice competed with BM MNCs from congenic (Ly5.1/Ly5.2) WT mice to reconstitute the haematopoietic compartment of an irradiated recipient mouse (Ly5.1). Flow cytometric analysis of peripheral blood of the transplanted recipients taken at 4 weeks after transplantation revealed that *Atm*$^{-/-}$ BM MNCs were just as able as the competitor cells to contribute to haematopoietic reconstitution (Fig. 1c, left panel). Thus, short-term repopulation was not affected. However, there were markedly fewer haematopoietic cells derived from *Atm*$^{-/-}$ BM MNCs than from competitor MNCs at 16 weeks after transplantation (Fig. 1c, right panel), indicating that *Atm*$^{-/-}$ HSCs lack long-term repopulating capacity. To examine this phenomenon more closely, we transplanted purified *Atm*$^{-/-}$ KSL cells into congenic recipients. We observed a marked impairment of long-term repopulation capacity (Fig. 1d), which affected the B, T and myeloid cell lineages (data not shown). These transplantation data did not result from altered homing or apoptosis of HSCs in the absence of ATM (Supplementary Fig. 2 and 3). Thus, ATM has an essential role in the self-renewal of adult HSCs but is less important for their proliferation or differentiation into haematopoietic progenitor cells.

The capacity for self-renewal under conditions of stress such as transplantation may or may not reflect the expansion of HSCs under normal homeostatic conditions. We therefore evaluated the effects of *Atm* deficiency on haematopoiesis in older mice. Although *Atm*$^{-/-}$ mice often die of lymphoma after 9 weeks of age[6–9], some lymphoma-free animals do survive. When we monitored haematopoiesis in these mice at 24 weeks of age, they all exhibited a progressive anaemia not seen in the WT mice (mean haemoglobin and haematocrit values at 24 weeks were 15.3 ± 0.94 g dl^{-1} and 50.3 ± 0.47%, respectively, in the WT ($n = 5$), in comparison with 9.93 ± 0.37 g dl^{-1} and 28.0 ± 1.41%, respectively, in *Atm*$^{-/-}$ mice ($n = 5$); Fig. 1e). The numbers of leukocytes and platelets in *Atm*$^{-/-}$ mice were also significantly lower than in the WT (mean white blood cell and platelet counts were 10,800 ± 210 μl^{-1} and 126 ± 19 × 10^4, respectively, in the WT ($n = 5$), in comparison with 7,300 ± 940 μl^{-1} and 76 ± 6 × 10^4, respectively, in *Atm*$^{-/-}$ mice ($n = 5$)). Analysis of BM from *Atm*$^{-/-}$ mice revealed a decrease in cellularity accompanied by a relative increase in adipose tissue (Fig. 1f; the mean ratio of number of BM MNCs from *Atm*$^{-/-}$ mice to that from WT mice was 0.37 ± 0.02). Neither cells with abnormal morphology nor lymphoma-like cells were observed in *Atm*$^{-/-}$ BM. Flow cytometric analysis of BM revealed that the absolute cell numbers of multiple lineages, including myeloid cells (Mac-1$^+$Gr-1$^+$), B cells (B220$^+$) and erythroid cells (Ter119$^+$ cells), were decreased in *Atm*$^{-/-}$ BM (Fig. 1g). Colony-forming assays confirmed that the numbers of myeloid and erythroid precursors among *Atm*$^{-/-}$ BM MNCs were markedly decreased (Supplementary Fig. 4a). Co-culture of BM MNCs on stromal cells showed that *Atm*$^{-/-}$ cells were no longer able to form any colonies after 2 weeks of culture (Supplementary Fig. 4b).

To analyse the HSC population in older *Atm*$^{-/-}$ mice in more detail, we examined the marker expression and colony-forming ability of the KSL fraction of *Atm*$^{-/-}$ BM cells. In contrast to the normal frequency of KSL cells observed in 8-week-old *Atm*$^{-/-}$ mice (Supplementary Fig. 1a), the c-Kit^{high} fraction of Sca-1$^+$Lineage$^-$ cells had disappeared in 24-week-old *Atm*$^{-/-}$ mice, and most c-Kit$^+$Sca-1$^+$Lineage$^-$ cells expressed only low levels of c-Kit

(Fig. 1h). It has been shown that the c-Kit^{high} fraction in Sca-1^{+}Lineage^{-} cells includes the long-term repopulating HSCs, and that c-Kit^{low} cells do not have this capacity[13]. Consistent with that report, our long-term culture of WT BM cells revealed that the c-Kit^{high} fraction, but not the c-Kit^{low} fraction, of the Sca-1^{+}Lineage^{-} contained HSCs (Supplementary Fig. 4c). As expected, the c-Kit^{low}Sca-1^{+}Lineage^{-} cells found in *Atm*$^{-/-}$ mice did not form any colonies in long-term cultures. Furthermore, repopulating cells derived from *Atm*$^{-/-}$ BM MNCs were no longer observed in recipient mice at either 4 or 16 weeks after transplantation (Supplementary Fig. 4d). Thus, our data indicate that chronic *Atm* deficiency *in vivo* results in progressive multi-lineage BM failure due to defective maintenance of the adult HSC pool.

To explain the mechanism underlying the regulation of the HSC pool by ATM, we investigated whether the defect in *Atm*$^{-/-}$ HSCs was caused by telomere dysfunction. The telomere length of BM cells was not affected by the loss of *Atm* alone (Supplementary Fig. 5). This result is consistent with a previous report showing that telomere dysfunction (as evaluated by anaphase bridging) was not observed in *Atm*$^{-/-}$ mice[5]. We also examined whether enhancement of telomerase activity could restore the repopulating capacity of *Atm*$^{-/-}$ HSCs. To this end, we used retroviral infection to introduce telomere reverse transcriptase (TERT) into *Atm*$^{-/-}$ KSL cells. However, overexpression of TERT was not able to rescue the defect (Table 1). These data indicate that ATM is required for the maintenance of HSC repopulation capacity in a telomere-independent manner.

In addition to telomere maintenance, it has been suggested that ATM might be involved in oxidative defence through the induction of the major anti-oxidative systems mediated by catalase, glutathione peroxidase, superoxide dismutase and glutathione reductase[14]. To determine whether the altered HSC function in *Atm*$^{-/-}$ mice was related to oxidative stress, we examined the concentration of reactive oxygen species (ROS) in HSCs. The intracellular concentration of H_2O_2, which was evaluated by 2′-7′-dichlorofluorescene diacetate (DCF-DA) staining, was higher in KSL cells from 8-week-old *Atm*$^{-/-}$ mice than from WT controls (Fig. 2a, left panel). The elevation of H_2O_2 in *Atm*$^{-/-}$ KSL cells was even more pronounced after 2 days of culture with stem cell factor (SCF) and thrombopoietin, which support HSC cell division[15]

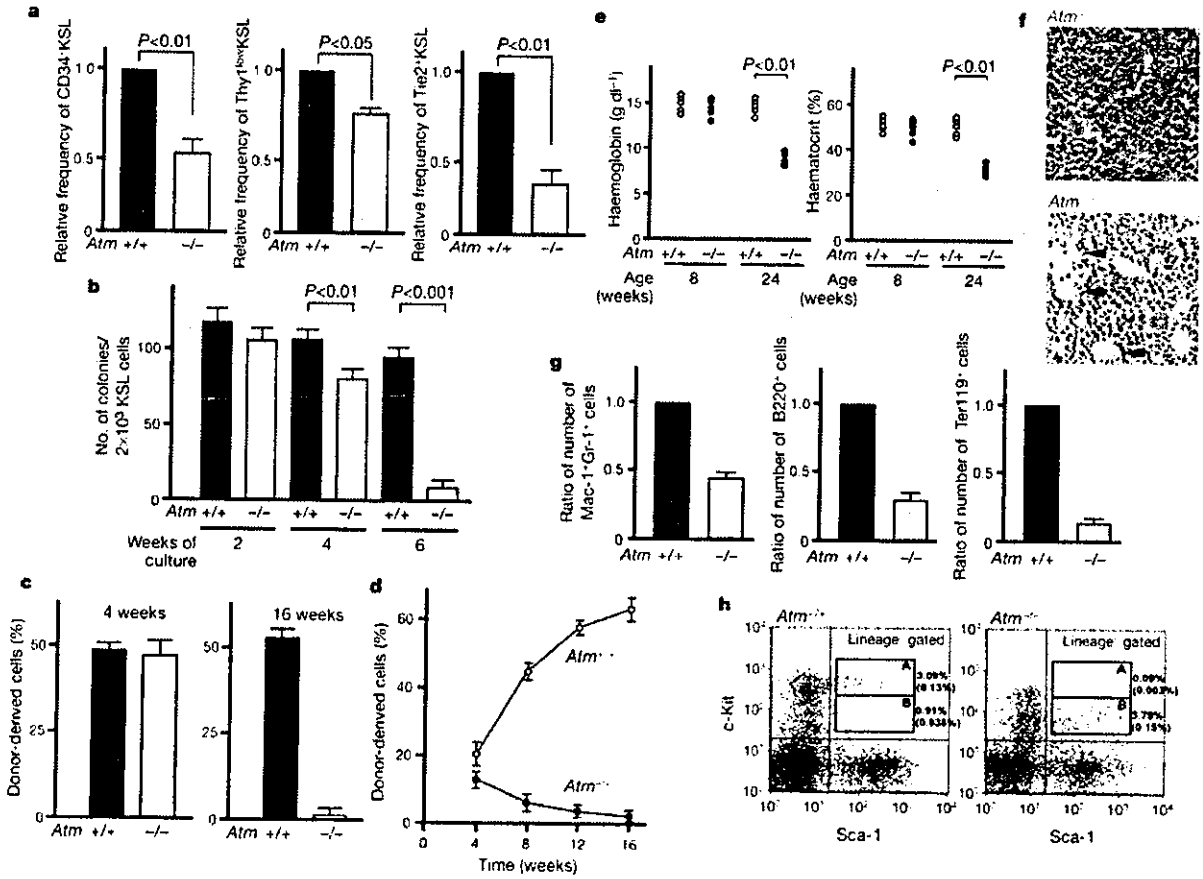

Figure 1 Defective haematopoiesis in the absence of ATM. **a**, Decreased frequencies of stem cell subsets. Results are mean relative frequencies ± s.d. for CD34^{-}KSL (left), Thy1^{low}KSL (middle) and Tie2^{+}KSL (right) cells in *Atm*$^{-/-}$ BM compared with *Atm*$^{+/+}$ BM ($n = 4$). **b**, Decreased colony formation after long-term culture of *Atm*$^{+/+}$ and *Atm*$^{-/-}$ KSL cells (2×10^3). Results are means ± s.d. ($n = 5$). **c**, **d**, Defective haematopoietic reconstitution. Recipient mice were transplanted with 4×10^5 BM MNCs (**c**) or 2×10^3 KSL cells (**d**) from *Atm*$^{+/+}$ or *Atm*$^{-/-}$ mice in competition assays. Results are mean percentages ± s.d. of donor-derived cells ($n = 5$). **e**, Concentrations of haemoglobin (left panel) and haematocrit (right panel) in peripheral blood of individual *Atm*$^{+/+}$ and *Atm*$^{-/-}$ mice of the indicated ages ($n = 5$). **f**, Decreased BM cellularity. Sections of BM from 24-week-old *Atm*$^{+/+}$ and *Atm*$^{-/-}$ mice were stained with haematoxylin and eosin. Arrows indicate adipose tissue. **g**, Decreased numbers of myeloid cells (left), B cells (middle) and erythroid cells (right) in *Atm*$^{-/-}$ BM. Results are mean relative frequencies ± s.d. of cells in *Atm*$^{-/-}$ BM compared with *Atm*$^{+/+}$ BM ($n = 4$). **h**, Decreased KSL cells in 24-week-old *Atm*$^{-/-}$ mice. For each panel, inset A shows c-Kit^{high}Sca-1^{+}Lineage^{-} cells and inset B shows c-Kit^{low}Sca-1^{+}Lineage^{-} cells. The frequencies of KSL cells as a percentage of total Lineage^{-} cells, and of total BM cells (in brackets) are indicated. Results are representative of four mice per genotype.

(Fig. 2a, right panel). In an effort to manipulate intracellular ROS concentrations, we treated WT and *Atm*$^{-/-}$ KSL cells with the permeant thiol *N*-acetyl-L-cysteine (NAC), which acts as an anti-oxidative agent[16]. Treatment of *Atm*$^{-/-}$ KSL cells with NAC significantly decreased the concentration of intracellular ROS (Fig. 2a, right panel).

To determine whether the defective repopulating capacity of *Atm*$^{-/-}$ mice could be restored by decreasing their elevated intracellular ROS, we established 6-week cultures of WT and *Atm*$^{-/-}$ KSL cells on stromal cells and treated them with one of the anti-oxidants NAC or catalase. The numbers of colonies formed from *Atm*$^{-/-}$ HSCs were restored to near-WT levels after treatment with either anti-oxidative agent (Fig. 2b). To replicate this phenomenon *in vivo*, we decreased the ROS in cells of 8-week-old *Atm*$^{-/-}$ mice by the daily subcutaneous administration of NAC (100 mg kg^{-1} d^{-1}) for 3 weeks. We found that the treatment of *Atm*$^{-/-}$ mice with NAC before transplantation improved haematopoietic reconstitution at 16 weeks after transplantation to a degree, but that total repopulation was still significantly lower than when WT KSL were used (Fig. 2c). Neither did NAC treatment of the recipient mice after transplantation with *Atm*$^{-/-}$ KSL cells completely rescue reconstitution. However, when NAC was administered both before and after BMT, the level of repopulation achieved was comparable to that of the WT. Treatment with NAC either before or after transplantation, or at both times, did not affect the repopulating capacity of WT HSCs in our system (Fig. 2c and data not shown). The rescued reconstitutive capacity of *Atm*$^{-/-}$ HSCs was confirmed by the detection of donor-derived B cells, T cells and myeloid cells in recipient mice (data not shown). These results show that the elevated ROS present in *Atm*$^{-/-}$ mice are the primary cause of the defective repopulating capacity of *Atm*$^{-/-}$ HSCs.

We next investigated whether long-term treatment with NAC could prevent BM failure in older *Atm*$^{-/-}$ mice. NAC was administered daily to 4-week-old WT and *Atm*$^{-/-}$ mice until they reached the age of 24 weeks. Although H_2O_2 concentrations in *Atm*$^{-/-}$ KSL cells were initially elevated over those in WT KSL cells, treatment with NAC decreased H_2O_2 concentrations to those in WT KSL cells

Table 1 Effects of TERT overexpression on haematopoietic reconstitution

Cell type	No. of mice showing reconstituted haematopoiesis (% of donor cells) EGFP	TERT
WT	4/4 (32–46%)	4/4 (35–48%)
Atm$^{-/-}$	0/4 (0%)	0/4 (0%)

KSL cells (5×10^3) were incubated with SCF and thrombopoietin and infected with retrovirus carrying TERT/EGFP or EGFP. The enhanced telomerase activity with exogenous TERT was confirmed by telomeric repeat amplification protocol assay. These cells (Ly5.2) were transplanted into Ly5.1 mice along with 4×10^5 Ly5.1 BM MNCs, which served as competitor cells. Haematopoietic reconstitution was confirmed by the detection of more than 1% donor-derived peripheral blood cells 16 weeks after transplantation. The infection efficiency of both retroviral vectors was 40–60% of WT and *Atm*$^{-/-}$ KSL cells as evaluated by detection of EGFP expression.

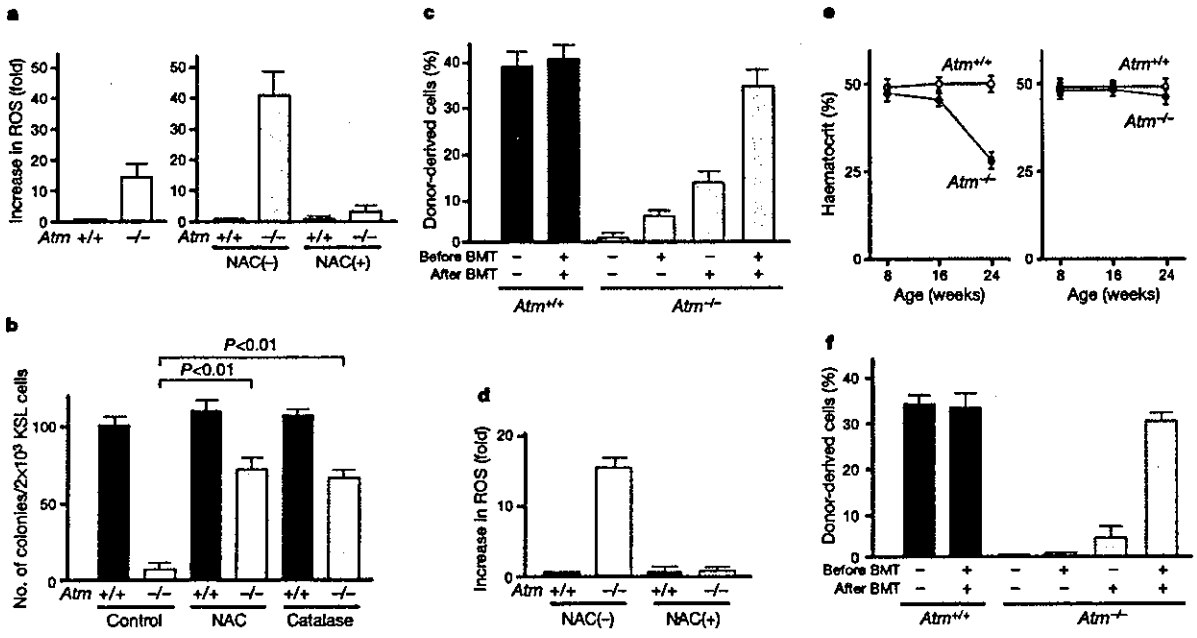

Figure 2 The defect in *Atm*$^{-/-}$ HSC function is caused by elevated ROS. **a**, Increased intracellular ROS. Left, H_2O_2 concentrations were determined by DCF-DA staining in freshly isolated KSL cells from 8-week-old *Atm*$^{+/+}$ and *Atm*$^{-/-}$ mice. Right, KSL cells were also incubated with cytokines alone or with cytokines plus the anti-oxidant NAC. Results are expressed as mean fold increases ± s.d. in intracellular ROS in cells in comparison with *Atm*$^{+/+}$ cells incubated with cytokines alone ($n = 5$). **b**, Restoration of colony formation after long-term culture with anti-oxidative agents. KSL cells were cultured for 6 weeks on OP9 stromal cells with or without 100 μM NAC or 100 U ml^{-1} catalase. Results are means ± s.d. ($n = 5$). **c**, Restored haematopoietic reconstitution *in vivo* with NAC treatment. KSL cells (5×10^3) were isolated from 8-week-old *Atm*$^{+/+}$ or *Atm*$^{-/-}$ mice that had been treated subcutaneously with NAC (100 mg kg^{-1} d^{-1}) for 3 weeks (indicated as 'before BMT'). Some recipient mice were also treated with NAC after transplantation ('after BMT'). Results are mean percentages ± s.d. of donor-derived cells at 16 weeks after transplantation ($n = 3$). **d**, Reduction in intracellular ROS *in vivo* with NAC treatment. H_2O_2 concentrations were determined in KSL cells from 24-week-old *Atm*$^{+/+}$ and *Atm*$^{-/-}$ mice that had been either left untreated or treated with NAC for 20 weeks. Results are mean fold increases ± s.d. in H_2O_2 in comparison with *Atm*$^{+/+}$ cells without NAC ($n = 3$). **e**, Prevention of anaemia by treatment with NAC. Mean concentrations ± s.d. of haematocrit in peripheral blood of untreated (left) or NAC-treated (right) *Atm*$^{+/+}$ and *Atm*$^{-/-}$ mice of the indicated ages are shown ($n = 4$). **f**, Restored haematopoietic reconstitution *in vivo* with long-term treatment with NAC. KSL cells (5×10^3) were isolated from 24-week-old *Atm*$^{+/+}$ or *Atm*$^{-/-}$ mice that had been treated with NAC for 20 weeks (indicated as 'before BMT'). Some recipient mice were also treated with NAC after transplantation ('after BMT'). Results are mean percentages ± s.d. of donor-derived cells at 16 weeks after transplantation ($n = 3$).

from 24-week-old *Atm*$^{-/-}$ mice, as expected (Fig. 2d). *Atm*$^{-/-}$ mice that received long-term treatment with NAC did not show anaemia (Fig. 2e), a decrease in progenitor colony-forming capacity (Supplementary Fig. 6a), or reduced frequencies of stem cell subsets (Supplementary Fig. 6b, c). We therefore concluded that the observed decrease in ROS prevented BM failure in older *Atm*$^{-/-}$ mice. Although the HSCs of older *Atm*$^{-/-}$ mice lose their repopulating capacity even when NAC is given to recipient mice after transplantation, a combination of long-term treatment with NAC both before and after transplantation completely rescued stem cell function (Fig. 2f). These results show that it is the elevation in ROS, and not some other factor, that causes the defect in *Atm*$^{-/-}$ stem cell function *in vivo*.

To understand better how the elevation in ROS affects *Atm*$^{-/-}$ HSCs, we used polymerase chain reaction with reverse transcription (RT–PCR) to compare the gene expression profiles of KSL cells freshly isolated from the BM of 8-week-old WT and *Atm*$^{-/-}$ mice. Several genes involved in the maintenance of the HSC compartment were analysed, including *HOXB4* (ref. 17), *Bmi-1* (refs 18, 19) and those encoding CDK inhibitors[20,21]. However, no obvious differences in gene expression were observed between WT and *Atm*$^{-/-}$ mice (Fig. 3a). We next attempted to mimic transplantation conditions by incubating KSL cells with cytokines *in vitro* for 2 days, followed by gene expression profiling. The tumour suppressors p16^{INK4a} and p19^{ARF}, which are generated by alternative splicing from the *INK4a* locus[22], were highly elevated in *Atm*$^{-/-}$ KSL cells under these conditions (Fig. 3b). In contrast, p21$^{WAF1/CIP1}$ and p27^{KIP1}, which are members of a different CDK inhibitor family, were not affected (Fig. 3b and data not shown). Treatment with NAC abrogated the upregulation of p16^{INK4a} and p19^{ARF} expression in *Atm*$^{-/-}$ KSL cells *in vitro* (Fig. 3b), indicating that the elevation of ROS that occurs in the absence of *Atm* controls p16^{INK4a} and p19^{ARF} expression as well as repopulating capacity. To investigate whether p16^{INK4a} and p19^{ARF} were similarly affected *in vivo*, we analysed gene expression profiles of immature haematopoietic cell populations (the KSL and Lineage$^-$ fractions) in 24-week-old *Atm*$^{-/-}$ mice with BM failure. The expression levels of both p16^{INK4a} and p19^{ARF} in *Atm*$^{-/-}$ cells were significantly higher than those in the WT (Fig. 3c and Supplementary Fig. 7). Furthermore, long-term treatment with NAC decreased the expression of p16^{INK4a} and p19^{ARF} in 24-week-old *Atm*$^{-/-}$KSL cells *in vivo* (Fig. 3d and Supplementary Fig. 7). Upregulation of p16^{INK4a} and p19^{ARF} by the loss of Bmi-1, a transcriptional repressor of the p16^{INK4a} and p19^{ARF} genes[23], led to defective self-renewal of adult HSCs and neural stem cells, but was less critical for the generation of the differentiated progeny of these cell types[18,19,24]. We therefore speculated that the increased ROS present in *Atm*$^{-/-}$ mice might cause the loss of the HSC pool through the upregulation of p16^{INK4a} and p19^{ARF}.

To test this hypothesis, we reduced p16^{INK4a} and p19^{ARF}

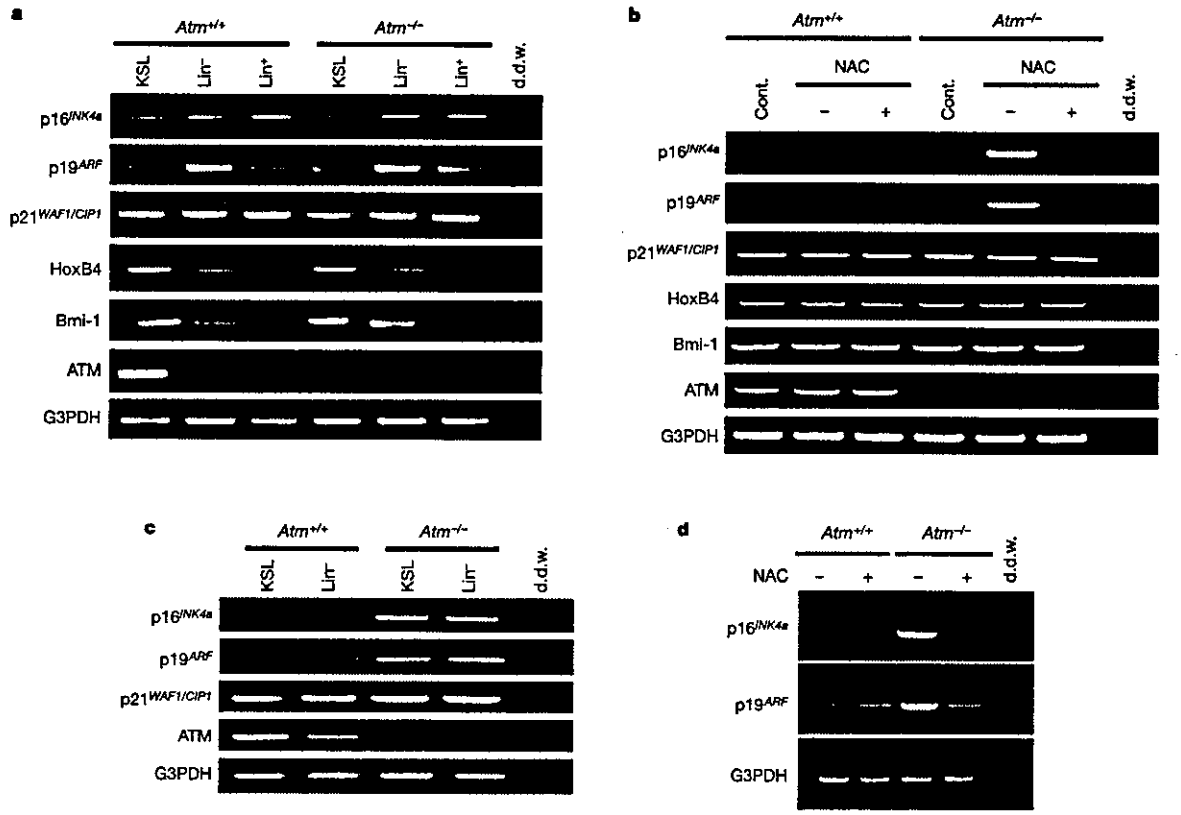

Figure 3 Elevated ROS induces upregulation of p16^{INK4a} and p19^{ARF} in *Atm*$^{-/-}$ KSL cells. **a**, Normal gene expression profile in haematopoietic fractions of 8-week-old *Atm*$^{-/-}$ mice. One result representative of at least three trials is shown. Lin, Lineage; d.d.w., double-distilled water. **b**, Upregulation of p16^{INK4a} and p19^{ARF} expression in cultured *Atm*$^{-/-}$ KSL cells *in vitro*. KSL cells were obtained from 8-week-old *Atm*$^{+/+}$ and *Atm*$^{-/-}$ mice, and gene expression profiles were determined in KSL cells that had been either freshly isolated (Cont.), incubated with cytokines alone (NAC −) or incubated with cytokines plus NAC (NAC +). **c**, Upregulation of p16^{INK4a} and p19^{ARF} expression in KSL cells from aged *Atm*$^{-/-}$ mice. Gene expression profiles of KSL cells from 24-week-old *Atm*$^{+/+}$ and *Atm*$^{-/-}$ mice are shown. **d**, Restoration of normal p16^{INK4a} and p19^{ARF} expression *in vivo* by NAC treatment. Gene expression profiles were determined in KSL cells from 24-week-old *Atm*$^{-/-}$ mice that had been either left untreated or treated with NAC for 20 weeks. G3PDH, glyceraldehyde-3phosphate dehydrogenase.

expression in KSL cells by the retroviral introduction of *Bmi-1*. Normalization of $p16^{INK4a}$ and $p19^{ARF}$ expression by the overexpression of Bmi-1 was confirmed by RT–PCR (Fig. 4a). Transplantation of WT KSL cells expressing either Bmi-1 or the control vector enhanced green fluorescent protein (EGFP) reconstituted donor-derived haematopoiesis in recipient mice. However, transplanted $Atm^{-/-}$ KSL cells could restore HSC repopulating capacity in the recipient only when the cells were infected with the Bmi-1-expressing retrovirus and not with the control EGFP-expressing retrovirus (Fig. 4b). These results indicated that upregulation of either $p16^{INK4a}$ or $p19^{ARF}$ causes the defective stem cell function observed in $Atm^{-/-}$ mice. It has been shown that upregulation of $p16^{INK4a}$ inhibits the phosphorylation of Rb family members (that is, it inhibits the inactivation of Rb function), whereas upregulation of $p19^{ARF}$ inhibits the degradation of p53 protein[22]. To identify which pathway, $p16^{INK4a}$–Rb or $p19^{ARF}$–p53, governs stem cell function, we inhibited the function of Rb family members or p53 by infecting $Atm^{-/-}$ KSL cells with a retroviral vector expressing human papilloma virus type 16 E7 and E6, respectively[25]. The overexpression of E7, but not E6, restored the repopulating capacity of $Atm^{-/-}$ HSCs, indicating that it is the $p16^{INK4a}$–Rb pathway that contributes to defective stem cell function in response to the elevated ROS in $Atm^{-/-}$ HSCs (Fig. 4c).

Haematopoietic progenitors have a high replicative potential and express telomerase to protect the ends of their chromosomes. As an animal ages, the telomeres undergo erosion. HSCs can also undergo telomere shortening, as reported in an examination of the serial transplantation of HSCs[26]. Accelerated telomere erosion due to the loss of Terc resulted in a decrease in the long-term repopulating capacity of these HSCs[27,28]. However, overexpression of TERT in mouse HSCs to prevent telomere erosion has no effect on the longevity of these cells[29], indicating that telomere-independent mechanisms might regulate the self-renewal of HSCs. Indeed, our study supports a model in which HSC self-renewal is regulated by ROS, which are in turn controlled by ATM (Fig. 4d). Although there are discrepancies between the phenotypes of patients with ataxia–telangiectasia and $Atm^{-/-}$ mice, we believe that our results shed light on a possible ATM function on the self-renewal of human stem cells and that the defect in HSC capacity might link to ataxia–telangiectasia pathophysiology. The recovery of HSC function by treatment with NAC indicates that patients with ataxia–telangiectasia might benefit from the administration of anti-oxidative agents as a pharmaceutical treatment. Our work could have repercussions outside the field of haematology, because the signalling pathways regulating stem cell self-renewal might also be used by cancer cells to drive malignant proliferation[30]. The idea leads to the intriguing notion that tumour suppressors might participate in the regulation of stem cell function. It supports a model in which master regulator molecules govern the disparate processes of stem cell self-renewal, normal ageing and tumour development. □

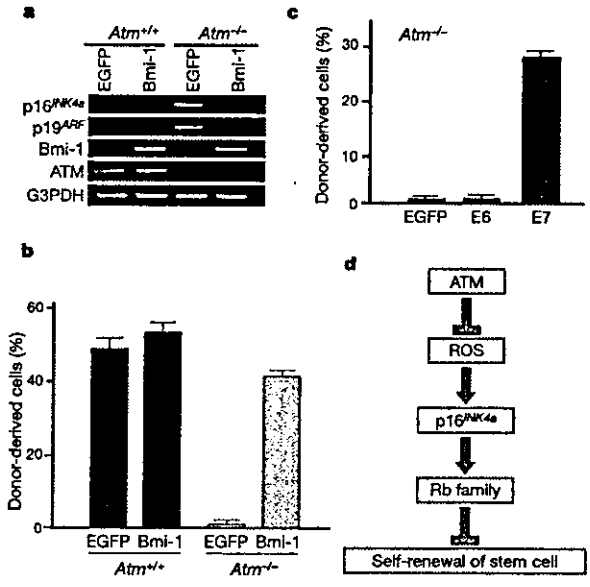

Figure 4 Activation of the $p16^{INK4a}$-Rb pathway causes the defect in stem cell function in $Atm^{-/-}$ mice. **a**, **b**, Restored haematopoietic reconstitution *in vivo* by overexpression of Bmi-1. KSL cells (5×10^3) isolated from 8-week-old $Atm^{+/+}$ or $Atm^{-/-}$ mice were infected with retrovirus carrying Bmi-1/EGFP or EGFP alone. The expression of $p16^{INK4a}$ and $p19^{ARF}$ in infected $EGFP^+$ KSL cells collected by flow cytometry were evaluated by RT–PCR (**a**). **b**, Recipient mice were transplanted with the $Atm^{+/+}$ or $Atm^{-/-}$ KSL cells from **a** in competition assays. Results are mean percentages ± s.d. of donor-derived cells at 16 weeks after transplantation ($n = 3$). **c**, Restored haematopoietic reconstitution *in vivo* by overexpression of E7. Recipient mice were transplanted in competition assays with $Atm^{-/-}$ KSL cells infected with retrovirus carrying either E6, E7 or EGFP as shown in **b** ($n = 3$). **d**, Proposed model for a role of ATM in the maintenance of HSC self-renewal.

Methods

Mice

$Atm^{+/-}$ mice were a gift from P. J. McKinnon (St Jude Children's Research Hospital, Memphis, Tennessee). Offspring of these mice were genotyped by PCR-based assays with mouse tail DNA. Littermates were used as controls in all experiments. C57BL/6 mice congenic for the Ly5 locus (B6-Ly5.1) were purchased from Sankyo-Lab Service.

Long-term cultures and colony-forming assays

For long-term cultures, BM MNCs or KSL cells were co-cultured with OP9 cells in MEM (Sigma) containing 12.5% fetal calf serum (JRH Bioscience), 12.5% horse serum (Gibco BRL) and 1 nM dexamethasone. After 2, 4 or 6 weeks of culture, cells were harvested and used for haematopoietic colony-forming assays. Methylcellulose colony-forming assays were performed with 20 ng ml^{-1} SCF (PeproTech EC Ltd), 20 ng ml^{-1} interleukin-3 (PeproTech EC Ltd), 2 U ml^{-1} erythropoietin (Chugai Pharmaceutical Co., Ltd) as described previously[22]. For some experiments, 100 μM NAC (Sigma) or 100 U ml^{-1} catalase (Sigma) was added to long-term cultures.

Flow cytometry

The following monoclonal antibodies (mAbs) were used for flow cytometric analyses: mAbs against c-Kit (2B8), Sca-1 (E13-161.7), CD4 (L3T4), CD8 (53-6.72), B220 (RA3-6B2), TER-119, Gr-1 (RB6-8C5), CD34 (RAM34), Thy1 (53-2.1), anti-Mac-1 (M1/70) and Tie2 (TEK4). All mAbs were purchased from BD. A mixture of mAbs against CD4, CD8, B220, TER-119, Mac-1 and Gr-1 was used as a lineage marker (Lineage).

Competitive reconstitution

Lethally irradiated C57Bl/6-Ly5.1 congenic mice were competitively reconstituted with 4×10^5 BM MNCs or KSL cells from $Atm^{+/+}$ or $Atm^{-/-}$ mice (Ly5.2), in competition with 4×10^5 BM MNCs from C57Bl/6-Ly5.1/5.2 mice. Reconstitution of donor (Ly5.2) myeloid and lymphoid cells was monitored by staining blood cells with antibodies against Ly5.2, Ly5.1, CD3, B220, Mac-1 and Gr-1.

Retroviral transduction

Retroviral gene transductions of cDNAs encoding mouse TERT, Bmi-1, E6 or E7 were performed with the retroviral vector pMY/IRES/EGFP. KSL cells (5×10^3) from $Atm^{+/+}$ or $Atm^{-/-}$ mice were incubated for 24 h with 100 ng ml^{-1} SCF and 100 ng ml^{-1} thrombopoietin followed by incubation for 48 h with retrovirus. The infected KSL cells were transplanted into lethally irradiated Ly5.1 mice along with 4×10^5 competitor BM MNCs. The efficiency of gene transduction was evaluated by expression of EGFP.

Analysis of intracellular ROS

NAC was dissolved in saline solution at pH 7.0. For experiments *in vivo*, mice were injected subcutaneously once daily with either NAC (100 mg kg^{-1}) or saline solution. For experiments *in vitro*, cell cultures were treated with 100 μM NAC. To assess the generation of ROS in KSL cells, freshly isolated KSL cells (5×10^3) were incubated for 2 days either with cytokines (100 ng ml^{-1} SCF and 100 ng ml^{-1} thrombopoietin) alone, or with cytokines plus 100 μM NAC. Samples of the cultures were loaded with 5 μM DCF-DA (Sigma) and incubated on a shaker at 37 °C for 30 min. The peak excitation wavelength for oxidized DCF was 488 nm and that for emission was 525 nm.

RT–PCR

cDNAs were reverse-transcribed from total RNA prepared from 5×10^3 KSL, Lineage$^-$ or Lineage$^+$ cells. For some experiments, cDNA was prepared from KSL cells that had been freshly isolated and incubated for 2 days with cytokines (100 ng ml^{-1} SCF and 100 ng ml^{-1} thrombopoietin) alone, or with cytokines plus 100 μM NAC. Primer sequences are shown in Supplementary Table 1.

Statistical analysis

P values were calculated by unpaired Student's *t*-test.

Received 13 July; accepted 30 August 2004; doi:10.1038/nature02989.

1. Meyn, M. S. Ataxia–telangiectasia and cellular responses to DNA damage. *Cancer Res.* **55**, 5991–6001 (1995).
2. Shiloh, Y. ATM and related protein kinases: safeguarding genome integrity. *Nature Rev. Cancer* **3**, 155–168 (2003).
3. Shiloh, Y. & Rotman, G. Ataxia–telangiectasia and the ATM gene: linking neurodegeneration, immunodeficiency, and cancer to cell cycle checkpoints. *J. Clin. Immunol.* **16**, 254–260 (1996).
4. Savitsky, K. *et al.* A single ataxia telangiectasia gene with a product similar to PI-3 kinase. *Science* **268**, 1749–1753 (1995).
5. Wong, K. K. *et al.* Telomere dysfunction and Atm deficiency compromises organ homeostasis and accelerates ageing. *Nature* **421**, 643–648 (2003).
6. Barlow, C. *et al.* Atm-deficient mice: a paradigm of ataxia telangiectasia. *Cell* **86**, 159–171 (1996).
7. Xu, Y. *et al.* Targeted disruption of ATM leads to growth retardation, chromosomal fragmentation during meiosis, immune defects, and thymic lymphoma. *Genes Dev.* **10**, 2411–2422 (1996).
8. Elson, A. *et al.* Pleiotropic defects in ataxia-telangiectasia protein-deficient mice. *Proc. Natl Acad. Sci. USA* **93**, 13084–13089 (1996).
9. Herzog, K. H., Chong, M. J., Kapsetaki, M., Morgan, J. I. & McKinnon, P. J. Requirement for Atm in ionizing radiation-induced cell death in the developing central nervous system. *Science* **280**, 1089–1091 (1998).
10. Osawa, M., Hanada, K., Hamada, H. & Nakauchi, H. Long-term lymphohematopoietic reconstitution by a single CD34-low/negative hematopoietic stem cell. *Science* **273**, 242–245 (1996).
11. Morrison, S. J. & Weissman, I. L. The long-term repopulating subset of hematopoietic stem cells is deterministic and isolatable by phenotype. *Immunity* **1**, 661–673 (1994).
12. Arai, F. *et al.* Tie2/angiopoietin-1 signaling regulates hematopoietic stem cell quiescence in the bone marrow niche. *Cell* **118**, 149–161 (2004).
13. Randall, T. D. & Weissman, I. L. Phenotypic and functional changes induced at the clonal level in hematopoietic stem cells after 5-fluorouracil treatment. *Blood* **89**, 3596–3606 (1997).
14. Barzilai, A., Rotman, G. & Shiloh, Y. ATM deficiency and oxidative stress: a new dimension of defective response to DNA damage. *DNA Repair (Amst.)* **1**, 3–25 (2002).
15. Ema, H., Takano, H., Sudo, K. & Nakauchi, H. *In vitro* self-renewal division of hematopoietic stem cells. *J. Exp. Med.* **192**, 1281–1288 (2000).
16. Yan, M. *et al.* The ataxia–telangiectasia gene product may modulate DNA turnover and control cell fate by regulating cellular redox in lymphocytes. *FASEB J.* **15**, 1132–1138 (2001).
17. Antonchuk, J., Sauvageau, G. & Humphries, R. K. HOXB4-induced expansion of adult hematopoietic stem cells *ex vivo*. *Cell* **109**, 39–45 (2002).
18. Park, I. K. *et al.* Bmi-1 is required for maintenance of adult self-renewing haematopoietic stem cells. *Nature* **423**, 302–305 (2003).
19. Lessard, J. & Sauvageau, G. Bmi-1 determines the proliferative capacity of normal and leukaemic stem cells. *Nature* **423**, 255–260 (2003).
20. Cheng, T. *et al.* Hematopoietic stem cell quiescence maintained by p21cip1/waf1. *Science* **287**, 1804–1808 (2000).
21. Yuan, Y., Shen, H., Franklin, D. S., Scadden, D. T. & Cheng, T. *In vivo* self-renewing divisions of haematopoietic stem cells are increased in the absence of the early G1-phase inhibitor, p18INK4C. *Nature Cell Biol.* **6**, 436–442 (2004).
22. Lowe, S. W. & Sherr, C. J. Tumor suppression by Ink4a-Arf: progress and puzzles. *Curr. Opin. Genet. Dev.* **13**, 77–83 (2003).
23. Jacobs, J. J., Kieboom, K., Marino, S., DePinho, R. A. & van Lohuizen, M. The oncogene and Polycomb-group gene bmi-1 regulates cell proliferation and senescence through the ink4a locus. *Nature* **397**, 164–168 (1999).
24. Molofsky, A. V. *et al.* Bmi-1 dependence distinguishes neural stem cell self-renewal from progenitor proliferation. *Nature* **425**, 962–967 (2003).
25. Munger, K. & Howley, P. M. Human papillomavirus immortalization and transformation functions. *Virus Res.* **89**, 213–228 (2002).
26. Allsopp, R. C., Cheshier, S. & Weissman, I. L. Telomere shortening accompanies increased cell cycle activity during serial transplantation of hematopoietic stem cells. *J. Exp. Med.* **193**, 917–924 (2001).
27. Allsopp, R. C., Morin, G. B., DePinho, R., Harley, C. B. & Weissman, I. L. Telomerase is required to slow telomere shortening and extend replicative lifespan of HSCs during serial transplantation. *Blood* **102**, 517–520 (2003).
28. Samper, E. *et al.* Long-term repopulating ability of telomerase-deficient murine hematopoietic stem cells. *Blood* **99**, 2767–2775 (2002).
29. Allsopp, R. C. *et al.* Effect of TERT over-expression on the long-term transplantation capacity of hematopoietic stem cells. *Nature Med.* **9**, 369–371 (2003).
30. Reya, T., Morrison, S. J., Clarke, M. F. & Weissman, I. L. Stem cells, cancer, and cancer stem cells. *Nature* **414**, 105–111 (2001).

Supplementary Information accompanies the paper on **www.nature.com/nature**.

Acknowledgements We thank H. Saya for helpful discussions, T. Kiyono for providing E6 and E7 cDNA, A. Iwama for providing mouse *Bmi-1* cDNA and virus, F. Ishikawa for providing mouse TERT cDNA, T. Kitamura for providing retroviral vector pMY, A. Ono for technical support, and M. Saunders for scientific editing. A.H. was supported by grants-in-aid from the Cancer Research and from the Stem Cell Research of the Ministry of Education, Science, Sports, and Culture, Japan. T.S. was supported by a grant-in-aid from the Research for the Future Program and the Specially Promoted Research of the Ministry of Education, Science, Sports, and Culture, Japan.

Competing interests statement The authors declare that they have no competing financial interests.

Correspondence and requests for materials should be addressed to A.H. (ahirao@sc.itc.keio.ac.jp) or T.S. (sudato@sc.itc.keio.ac.jp).

Gfi-1 restricts proliferation and preserves functional integrity of haematopoietic stem cells

Hanno Hock[1,2,3], Melanie J. Hamblen[1,4], Heather M. Rooke[1,4], Jeffrey W. Schindler[1], Shireen Saleque[1], Yuko Fujiwara[1,4] & Stuart H. Orkin[1,3,4]

[1]Division of Hematology/Oncology, Children's Hospital, [2]Department of Medical Oncology and [3]Department of Pediatric Oncology, Dana Farber Cancer Institute, Harvard Medical School and the [4]Howard Hughes Medical Institute, Boston, Massachusetts 02115, USA

Haematopoietic stem cells (HSCs) sustain blood production throughout life. HSCs are capable of extensive proliferative expansion, as a single HSC may reconstitute lethally irradiated hosts[1]. In steady-state, HSCs remain largely quiescent and self-renew at a constant low rate, forestalling their exhaustion during adult life[2,3]. Whereas nuclear regulatory factors promoting proliferative programmes of HSCs *in vivo* and *ex vivo* have been identified[4–6], transcription factors restricting their cycling have

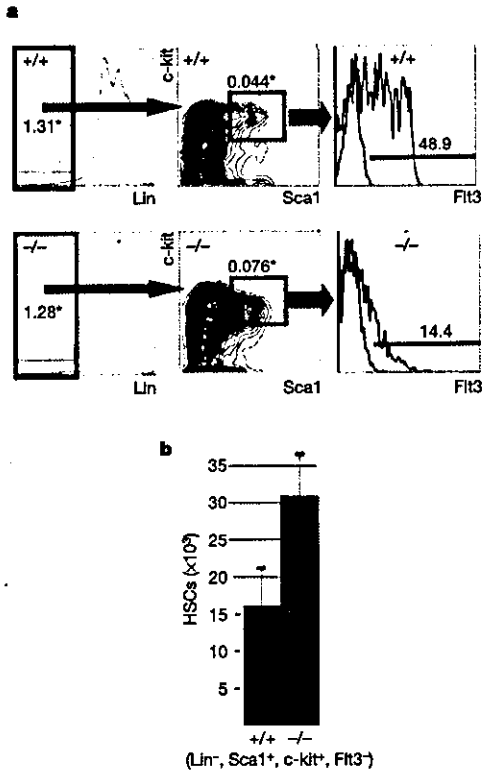

Figure 1 Immunophenotypic analysis of HSCs in *Gfi-1* $^{-/-}$ mice. **a**, Frequency of Lin$^-$, Sca1$^+$, c-kit$^+$ cells is elevated in *Gfi-1* $^{-/-}$ (−/−) mice compared with wild-type littermates (+/+). Left plots show lineage gates; standard deviation (s.d.): +/+ = 0.185, −/− = 0.16. Asterisks indicate percentage of bone marrow. Middle plots identify Lin$^-$, Sca1$^+$, c-kit$^+$ cells; s.d.: + /+ = 0.0045, −/− = 0.0016. Right plots demonstrate that Flt3 expression (red; isotype-matched control is black) within Lin$^-$, Sca1$^+$, c-kit$^+$ cells is reduced in *Gfi-1* $^{-/-}$ mice; s.d.: + /+ = 3.8, −/− = 2.9. Plots from one representative animal of four are shown; numbers are averages (n = 4). **b**, Total number of long-term repopulating HSCs, as average per animal (two tibia and fibula) and s.d. (n = 4), age ~4 weeks.

J. Radiat. Res., 45, 245–251 (2004) Regular Paper

Spontaneous and Radiation-induced Leukemogenesis of the Mouse Small Eye Mutant, *Pax6*^{Sey3H}

Yumiko NITTA[1]*, Kazuko YOSHIDA[2], Kenichi SATOH[3], Kei SENBA[4], Naomi NAKAGATA[5], Jo PETERS[6] and Bruce M. CATTANACH[6]

Chromosome deletion/Acute myeloid leukemia/^{60}Co gamma rays/Mouse small eye mutant/*Pax6*^{Sey3H}.

Allelic loss on the chromosome 2 is associated with radiation-induced murine acute myeloid leukemia. However, the gene, which contributes mainly to the leukemogenesis has not yet been identified. Expecting any predisposition to acute myeloid leukemia, we performed a radiation leukemogenensis experiment with *Pax6*^{Sey3H}, one of the small eye mutants carrying a congenital hemizygosity of the chromosome 2 middle region. A deletion mapping of *Pax6*^{Sey3H} with 50 STS markers indicated that the deleted segment extended between the 106.00 and 111.47 Mb site from the centromere with a length of 5.47 Mb. In the deleted segment, 6 known and 17 novel genes were located. *Pax6*^{Sey3H} mutants that crossed back into C3H/He did not develop myeloid leukemia spontaneously, but they did when exposed to gamma-rays. The final incidence of myeloid leukemia in mutants (25.8%) was as high as that in normal sibs (21.4%). Survival curves of leukemia-bearing mutants shifted toward the left ($p = 0.043$ by the Log rank test). F1 hybrids of *Pax6*^{Sey3H} with JF1 were less susceptible to radiation than *Pax6*^{Sey3H} onto C3H/He in regard to survival ($p = 0.003$ and $p < 0.00001$ for mutants and normal sibs, respectively, by a test of the difference between two proportions). Congenital deletion of the 5.47 Mb segment at the middle region on chromosome 2 alone did not trigger myeloid stem cells to expand clonally *in vivo*; however, the deletion shortcut the latency of radiation-induced myeloid leukemia.

INTRODUCTION

It is well known that leukemia occurs more frequently among atomic bomb survivors than in the general population.[1–3] Clinical, cytogenetic, and molecular-genetic examinations indicated that complex chromosome abnormalities without a specific type of translocation and a high incidence of genetic instability of leukemic cells were characteristic to radiation-related acute myeloid leukemia in humans.[4]

To clarify the mechanism of leukemogenesis, the experimental model is useful. Hayata *et al.* reported the high susceptibility of C3H/He mice to myeloid leukemia and the consistent occurrence of the deleted chromosome 2 in mouse myeloid leukemias.[5,6] Since this publication, there have been three independent articles that demonstrated the occurrence of the deleted chromosome 2 in mouse radiation-induced acute myeloid leukemia).[7–9] Alexander *et al.* reported the commonly deleted region of 6.5 cM from markers *D2Mit214* to *D2Mit395*, where *Wt1* and *Pax6* genes located.[7] Silver *et al.* reported the minimal deleted region for radiation-induced acute myeloid leukemia on chromosome 2.[8] The interval was 1 cM between markers *D2Mit126* and *D2Mit185*, in which *Wt1* and *Pax6* genes were involved. The genes flanking the SFFV proviral integration 1 (*Sfpi1*) were suggested to work tumor suppressive in leukemogenesis in accordance with the observation of homozygous deletion. Rithidech *et al.* reported another commonly deleted region on chromosome 2.[9] The interval was 4.6 cM between *D2Mit272* and *D2Mit394*, in which *Wt1* and *Pax6* genes existed.

WAGR (*Wilms'* tumor, aniridia, genitourinary anomalies, mental retardation) syndrome is one of the well-known congenital disorders, patients of which have carried the simultaneous deletion of *PAX6* and *WT1* (OMIM#194072). Mouse small eye mutants, *Pax6*^{Sey1H}, *Pax6*^{Sey2H}, and *Pax6*^{Sey3H} are animal models of the WAGR syndrome, characterized by the genomic deletion at the two genes' locus and by the small eye

*Corresponding author: Phone/Fax: +81-82-257-5877,
E-mail: yumiko@hiroshima-u.ac.jp
[1]International Radiation Information Center, Research Institute for Radiation Biology and Medicine, Hiroshima University, Kasumi, Minami-ku, Hiroshima 734-8553, Japan; [2]Radiation Hazards Research Group, National Institute for Radiological Science, Anagawa, Inage-ku, Chiba 263-8555, Japan; [3]Division of Bio-Medical Informatics, Research Institute for Radiation Biology and Medicine, Hiroshima University, Kasumi, Minami-ku, Hiroshima 734-8553, Japan; [4]Division of Developmental Genetics, Institute of Molecular Embryology and Genetics, Kumamoto University, 2-2-1 Honjo, Kumamoto 860-0811, Japan; [5]Divigion of Reproductive Engineering, Institute of Resource Development and Analysis, Kumamoto University, 2-2-1 Honjo, Kumamoto 860-0811, Japan; and [6]Mammalian Genetics Unit, Medical Research Council, Harwell, Didcot, OXON OX11 0RD, UK.

phenotype.[10] It is of great interest whether the congenital deletion of *Wt1* and *Pax6* predisposes mice to acute myeloid leukemia. If deletion mutants developed acute myeloid leukemia, and if any mutation was found in the monoallelic genes of myeloid leukemia cells, it could be possible to identify the gene responsible for leukemogenesis. Therefore we have tested the susceptibility of *Pax6^{Sey3H}* to radiation by using the established system for the induction of acute myeloid leukemia.[11]

MATERALS AND METHODS

Mice

Frozen embryos of the *Pax6^{Sey3H}* hemizygous mutant were purchased from MRC (Harwell, OXON, UK), and mutants have been maintained by crossing with C3H/He (Charles River Japan Inc.).[12] Offspring from the third generation were used for experiments. F1 hybrids backcrossed with C57BL/6N, BALB/C (Charles River Japan Inc.), or JF1 (National Institute of Genetics, Mishima, Japan) were used for deletion mapping. *Pax6^{Sey3H}* mice of the 3rd and 4th generations (C3H × *Pax6^{Sey3H}*) and F1 hybrid mice between *Pax6^{Sey3H}* and JF1 (JF1 × *Pax6^{Sey3H}*) were used for the tumorigenesis experiment.

Animal studies were carried out under guidance issued by the Research Institute for Radiation Biology and Medicine in Responsibility in the Use of Animals for Research.

Pax6^{Sey3H} was selected for testing because the deleted region was shortest among the three small eye mutants according to the previous report based on the cytogenetic examination.[10] The mutant with the shortest deletion was endowed with high fertility and viability. These two factors were very important for the completion of the carcinogenesis experiments using mutant mice.

Genotyping the mutant

DNA was prepared from the tail tips by use of a DNA rapid extraction kit (Qiagen, Hilden, Germany). The SSLP markers used were Mit markers. The marker set used was *D2Mit354, D2Mit219, D2Mit435, D2Mit183, D2Mit436, D2Mit220, D2Mit126, D2Mit14, D2Mit15, D2Mit302, D2Mit253, D2Mit186, D2Mit351, D2Mit350, D2Mit386, D2Mit303, D2Mit141, D2Mit221, D2Mit385, D2Mit184, D2Mit437, D2Mit249, D2Mit251, D2Mit250, D2Mit477, D2Mit333, D2Mit42, D2Mit99, D2Mit442, D2Mit387, D2Mit185, D2Mit128, D2Mit100, D2Mit206, D2Mit211, D2Mit58, D2Mit480, D2Mit482, D2Mit207, D2Mit102, D2Mit103, D2Mit398, D2Mit278, D2Mit487, D2Mit304, D2Mit224, D2Mit258, D2Mit78, D2Mit353* and *D2Mit13*. The sequence was obtained from the Whitehead Institute for Biomedical Research/MIT Center for Genome Research (http://www.genome.wi.mit.edu/), and their primers were obtained from Greiner Bio-One Ltd., Japan. The cycling conditions for the PCR were 40 × (1 min at 95°C, 1 min at 42°C, and 2 min at 72°C).[12] Aliquots of the 10 micro l of products were separated by electrophoresis on the 3% agarose gel.

Tumorigenicity test

The gamma-irradiation emitted from the ^{60}Co source (Shimadzu, Japan) was performed on the whole body at the age of 10 weeks. The exposure was single with a dose of 3.0 Gy at a rate of 68.7 cGy/min.[11] The tumorigenicity has been observed for 24 months.

Histopathological analysis.

The mice were autopsied when moribund, exhibiting anemia with palpable spleens, or at the age of termination, 24 months. The main organs and tumor tissues were fixed in 10% phosphate-buffered formalin, dehydrated with alcohol, embedded in paraffin wax, sectioned 4 micro m thick, stained with hematoxylin and eosin, and observed pathologically. The intestines from stomach to colon were sliced into serial sections 4 micro m thick for the examination of tumor multiplicity.

A standard avidin-biotin complex technique was performed for the peroxidase in the hematopoietic tumor cells in liver.[13] Polyclonal antibodies to peroxidase (MBL Inc., Japan) were used as the primary antibody at a titer of 1:1000.

Statistical analysis

Survival curves were prepared by the Kaplan-Meier method.[14] The difference between survival curves was evaluated by use of the Log rank and Wilcoxson test. Survival proportions and incidences of tumors at the age of 24 months were compared statistically by a test of the difference between two proportions.

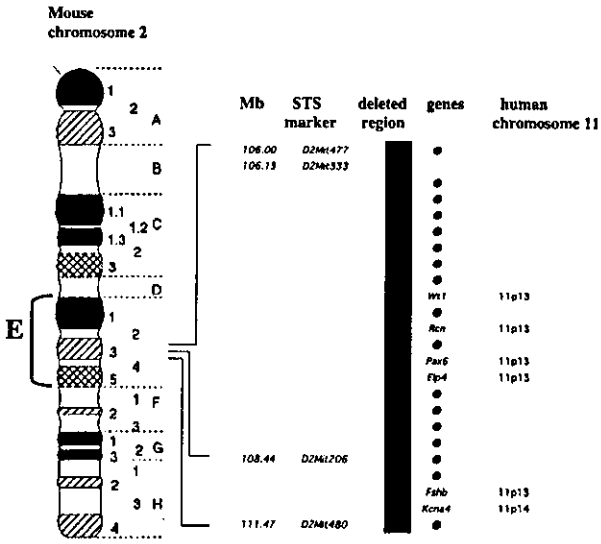

Fig. 1. The cytogenetic map of chromosome 2 combined with the genomic map of the deleted segment of *Pax6^{Sey3H}*. Base number was counted from centromere. Circles, indicated novel genes.

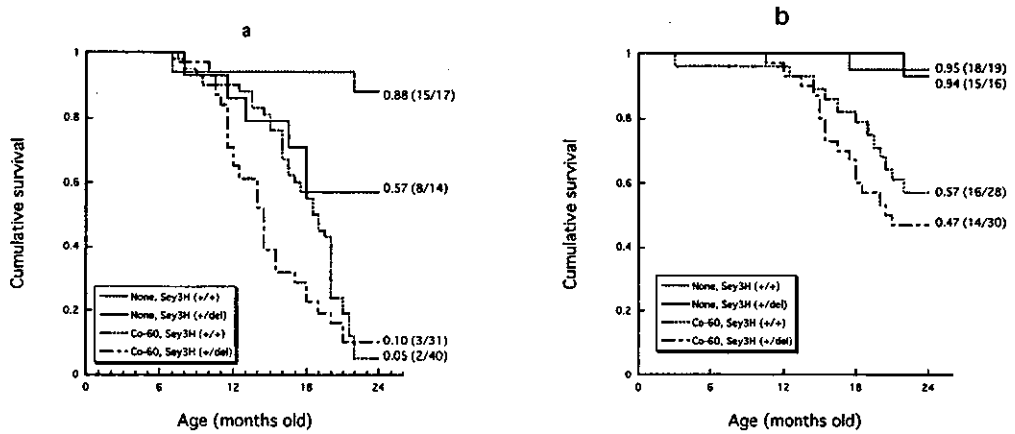

Fig. 2. a: Nonparametric Kaplan-Meier survivals of (C3H × of *Pax6*^{Sey3H}) mice. Numerical characters in the figure represent cumulative survival ratios at the age of 24 months: 0.88, 0.57, 0.05, and 0.10 for non-treated normal sibs, non-treated mutants, gamma-irradiated normal sibs, and gamma-irradiated mutants, respectively. The difference between the curve of gamma-irradiated mutants (— · —) and that of gamma-irradiated normal sibs (— -- —) was significant by the Wilcoxson test ($p = 0.006$). b: Nonparametric Kaplan-Meier survival curves of (JF1 × *Pax6*^{Sey3H}) mice. Numerical characters in the figure represent survival proportions at the age of 24 months: 0.94, 095, 0.57, and 0.47 for non-treated normal sibs, non-treated mutants, gamma-irradiated normal sibs, and gamma-irradiated mutants, respectively.

Table 1. Tumor spectrum of *Pax6*^{Sey3H} mice.

Genetic background (%)	C3H/He (93.5≤)				JF1 (50.0)			
Treatment	None		Co-60		None		Co-60	
Genotype[a]	+/del	+/+	+/del	+/+	+/del	+/+	+/del	+/+
Number of mice examined	14	17	31[c]	42[d]	16	19	30	28
Number of mice bearing tumors	5	5	25	32	2	0	22	12
Number of tumors observed	5	5	28	33	2	0	25	12
Hematopoietic systems (%)	0	1 (5.9)	14 (45.2)	11 (26.2)	0	0	3 (10.0)	2 (7.1)
Intestinal tract (%)	4 (28.6)	0	8 (25.8)[e]	0	0	0	6 (20.0)	1 (3.6)
Pancreas (%)	0	0	0	0	0	0	3 (10.0)	0
Liver (%)	1 (7.1)	3 (17.6)	4 (12.9)	10 (23.8)	2 (12.5)	0	7 (23.3)	7 (25.0)
Others (%)[b]	0	1 (5.9)	2 (6.5)	12 (28.6)	0	0	6 (20.0)	2 (7.1)

[a]+/del, hemizygous mutants; +/+, normal sibs. [b]Included tumors in the lung, ovary, and soft tissue. The percent of each tumor was given by [number of tumor-bearing mice/total number of mice] × 100. [c]Five mice (3 females and 2 males) autopsied before 24 months of age did not carry tumors. Atrophy of the spleen (2 cases), pancreatitis (2 case), and fatty degeneration of the pancreas (1 case) have been observed. [d]Ten mice (6 females and 4 males) autopsied or necropsied before 24 months of age did not carry tumors. Two males were found dead. Causes of their death were unknown. Atrophy of the spleen (2 cases), abdominal nodule of the degenerated adipose tissue (1 case), ovarian cysts (2 cases), endometrial cysts (2 cases), and hydronephrosis (1 case) have been observed. [e]$p = 0.002$ when the differences of tumor proportions between mutants and normal sibs were compared.

RESULTS

Deletion region of the mutant

Deletion mapping was performed to define the deleted ends. The deleted segment was between markers *D2Mit477* and *D2Mit480* (Fig. 1). The interval was 5.47 Mb between 106.00 Mb and 111.47 Mb from the centromere, in which the six known *Wilms'* tumor 1 (*Wt1*), reticulocarbin (*Rcn*), paired box gene 6 (*Pax6*), elongation protein homolog 4 (*Elp4*), follicular stimulation hormone beta (*Fshb*), and potassium channel voltage-gated shaker-related super family 4 (*Kcna4*) and 17 novel genes located (http://www.ensembl.org/Mus_musculus/geneview). The deleted segment of *Pax6*^{Sey3} was found to be longer than that previously reported (http://mrcseq.har.mrc.ac.uk/chr2map.html) by 2.27 Mb. Five genes, *Fshb*, *Kcna4*, and three novel genes, located within the segment (Fig. 1).

Myeloid leukemogenicity of (C3H × Pax6^{Sey3H}*) mutants*

Survival proportions at the age of 24 months were 0.57 and 0.88 for mutants and normal sibs, respectively, in non-treated groups (Fig. 2-a) (not statistically significant). The final survival proportion for mutants (0.10) was not different from that

Table 2. Pathological diagnosis of hematopoietic tumors in *Pax6*^{Sey3H} mice.

Genetic background (%)	C3H/He (93.5≤)				JF1 (50.0)			
Treatment	None		Co-60		None		Co-60	
Genotype (number of mice)[a]	+/del (14)	+/+ (17)	+/del (31)	+/+ (42)	+/del (16)	+/+ (19)	+/del (30)	+/+ (28)
Thymic lymphoma (%)[b]	0	0	3 (9.7)	1 (2.4)	0	0	1 (3.3)	0
Nonthymic lymphoma (%)	0	1 (5.9)	3 (9.7)	0	0	0	0	1 (3.6)
Myeloid leukemia (%)	0	0	8 (25.8)	9 (21.4)	0	0	2 (6.7)	1 (3.6)
Erythroleukemia (%)	0	0	0	1 (2.4)	0	0	0	0

[a]+/del; hemizygous mutants, +/+; normal sibs. [b]% was given by (number of tumor bearing mice/total number of mice) × 100.

Table 3. Tumor latencies.

Groups	Genetic background (%)	C3H/He (93.5≤)				JF1 (50.0)			
	Treatment	None		Co-60		None		Co-60	
	Genotype	+/del	+/+	+/del	+/+	+/del	+/+	+/del	+/+
Tumor latency[a] (days, mean ± SD)	Hematopoietic tumors[b]	–	–	348.3 ± 101.0	472.1 ± 119.2	–	–	320.3 ± 63.3	356
	Myeloid leukemia	–	–	342.5 ± 114.7[c]	464.2 ± 126.2	–	–	356	310
	Hematopoietic tumors except myeloid leukemia	–	–	314.2 ± 88.8	508.0 ± 107.7	–	–	249	402
	Intestinal tumor	295	–	401.5 ± 134.5	–	–	–	456.3 ± 49.0	568

[a]Latencies (mean ± SD) of mice autopsied before 24 months of age. [b]Including myeloid leukemia. [c]$p = 0.043$ when compared to normal sibs by the Log rank test.

Table 4. Sex bias on myeloid leukemogenesis.

Groups		Number of tumors	Tumor incidence (%) per:			Tumor latency (days, mean ± SD)
Genotype (number of mice)	Sex (number of mice)		Genotype group[a]	Sex	Genotype group (sex ratio-adjusted)[b]	
+/+ (42)	Female (18)	3	21.4	16.7	20.8	482.4 ± 131.4
	Male (24)	6		25.0		454.7 ± 135.3
+/del (31)	Female (19)	6	25.8	31.6	24.1	333.0 ± 132.2
	Male (12)	2		16.7		371

[a]Number of tumor-bearing mice/total number of mice. [b]Average of tumor incidences of the females and males.

of the normal sibs (0.05) in the gamma-irradiated groups. However, the survival curve of the mutants shifted toward the left with the higher decrease of survival proportion at young ages ($p = 0.006$ by the Wilcoxson test). There was no bias of sex on any survival curve in Fig 2-a.

Mutant mice did not develop hematopoietic tumors spontaneously, but they did when γ-irradiated (Table 1). The development of myeloid leukemia was radiation specific, and the final incidence of myeloid leukemia for mutants (25.8%) was as high as that for normal sibs (21.4%) (Table 2). The cumulative survival curve of mutants bearing myeloid leukemias shifted toward the left when compared to that of normal sibs ($p = 0.043$ by the Log rank test) (Table 3). The mean latencies of myeloid leukemia were 342.5 and 464.2 days for mutants and normal sibs, respectively.

There was no bias of sex on any survival curve; however, myeloid leukemias developed in female mutants with a high incidence (6 out of 8, or 75.0%) (Table 4). The incidences of myeloid leukemia in a comparison between sex-adjusted and non-adjusted, values were similar. The mean latency of myeloid leukemia for female mutants (330.0 days) was short.

Myeloid leukemoginicity of (JF1 × Pax6^{Sey3H}*) mutants*

The survival proportion of mutants was as high as that of normal sibs at the age of 24 months in the non-treated and gamma-irradiated groups (Fig. 2-b). Spontaneous hematopoietic tumors were not observed (Table 1). The incidences of myeloid leukemia were 6.7% and 3.6% for mutants and normal sibs, respectively, in the gamma-irradiated groups (Table 2).

With regard to the genetic background in normal sibs, the survival proportion of gamma-irradiated (JF1 × *Pax6*^{Sey3H}) at 24 months of age (0.57) was higher than that of irradiated (C3H × *Pax6*^{Sey3H}) (0.05) ($p < 0.00001$ by a test of the differ-

Table 5. A comparison of commonly deleted regions on mouse chromosome 2.

Reference (number)	Genetic background	Number of leukemia examined (deleted/total)	Chromosome 2 deletion						
			Chromosome		STS marker		Marker position (Mb)[c]		Length (Mb)[c]
			Band	Length (cM)	Proximal end	Distal end	Proximal end	Distal end	
Hayata (6)	C3H/He	49/52	C, D	–	–	–	–	–	–
Alexander (7)	SJL/J × CBA	22/22	D–E4	6.5	*D2Mit214*	*D2Mit395*	85.5	121.1	35.6
Silver (8)	CBA, C3H	5/5	C2–H4	1.0	*D2Mit126*	*D2Mit185*	85.5	107.0	21.5
Rithidech (9)	BALB/cJ × CBA/CaJ	8/8	D–E	4.6	*D2Mit272*	*D2Mit394*	91.8	118.7	26.9
Ban (16)	C3H/He[b]	2/2	E1[c]	–	*D2Mit15*	–	93.1	–	0.1
Nitta (12)	C3H/He	97/105	E1[c]	–	*D2Mit15*	–	93.1	–	0.1
Pax6^{Sey3H} (a)	101 × C3H/He	–	E3[c]	–	*D2Mit477*	*D2Mit480*	106.0	111.5	5.5

[a]Present manuscript. [b]Carrying a null mutation in one allele of the *Trp53* gene. [c]from web (http://www.ensembl.org/Mus_musculus/geneview).

ence between two proportions) (Fig. 2-a and b). Also, the survival proportion of gamma-irradiated (JF1 × *Pax6*^{Sey3H}) mutants (0.47) was higher than that of (C3H × *Pax6*^{Sey3H}) (0.10) ($p = 0.003$ by a test of the difference between two proportions).

Intestinal tumorigenicity of the mutant

The mutants of (C3H × *Pax6*^{Sey3H}) developed intestinal tumors spontaneously (Table 1). Because these tumors were found at the age of 24 months without any clinical sign (3 of 4 cases, or 75%), the development of these tumors had no influence on the survival proportion. Radiation did not raise the incidence of intestinal tumors in mutants, nor did it induce the tumors in normal sibs (Table 1). Tumor latencies were not comparable because the number of mice that developed the tumor before the age of 24 months was only one (Table 3). Cumulative survival curves drawn by the Kaplan-Meier method with the parameter of intestinal tumors showed no statistically significant difference between the non-treated and the gamma-irradiated groups (data not shown).

In cases of the (JF1 × *Pax6*^{Sey3H}) mutants, intestinal tumors were found when gamma-irradiated (Table 1). Three of 6 cases (50%) were found at 24 months of age with no clinical sign.

No case developed with both myeloid leukemia and intestinal tumors simultaneously (Table 1).

DISCUSSION

After the complete sequence of mouse genome in 2002, it became possible to get the positional information for each gene or each STS marker on each chromosome (http://www.ensembl.org/Mus_musculus/geneview). Table 5 summarizes the genomic information about the deleted segments of chromosome 2 associated with mouse acute myeloid leukemia. The congenitally deleted segment of *Pax6*^{Sey3H} was found to cover 15.4–25.6% of deleted segments reported in the radiation-induced myeloid leukemia.[7–9] Our result indicated that a congenital hemizygosity of the short segment of *Pax6*^{Sey3H} alone was not enough for the development of myeloid leukemias. When the hypothesis that the tumor suppressor gene controls the radiation-induced myeloid leukemogenesis is supported, no gene responsible for leukemogenesis is within the deleted region.

Another hypothesis for mouse radiation leukemogenesis is that the radiation-induced genetic instability is causal.[15–17] Under this viewpoint, the length of or genes in the hemizygous segment must be considerable. As the segment of 5.47 Mb occupied the utmost 3.02% of the whole genome of chromosome 2 (181.11 Mb), the length could be too short to force chromosomes unstable. There are several genes whose haploinsufficiency caused chromosomal instability.[18–20] The partial deletion of chromosome 2 observed in leukemia cells from mutant mice with a null mutation in one allele of the *Trp53* gene could be explained as an example of chromosomal instability caused by the *Trp53* haploinsufficiency (Table 5).[16]

It was unclear whether the shortening of leukemia latency observed in gamma-irradiated mutants was extraneous to or coincidental with the shortening of lifespans. However, when the values were compared by sex, a high incidence and a short latency of myeloid leukemia were found in female mutants. In consideration of the higher susceptibility in males than in females having resulted in the same system of radiation-induced myeloid leukemogenesis,[21] the cause of this reverse susceptibility in *Pax6*^{Sey3H} was speculated as follows. *Pax6*^{Sey3H} mutants could be susceptible to radiation-induced myeloid leukemogenesis. A much higher frequency in male mutants than in females (31.6%) had been expected; however, it was inhibited by another factor, such as the epigenetic status of the chromosome. The deleted allele of *Pax6*^{Sey3H} was paternal in the present experiment. Therefore the epigenetic status of the monoallelic region as well as the whole chromosome 2 in mutants should be different from those in normal sibs.

Unfortunately, a trial to produce *Pax6*^{Sey3H} carrying the maternally transmitted mutated allele failed. Because the fer-

tility of the *Pax6*^{Sey3H} female was very low, it took a long time to get a proper number of mutants for testing. Furthermore, the mortality of newborn mutants was high because of the growth retardation during embryogenesis. A kind of haploinsufficiency of the *Fshb* gene locating within the monoallelic segment (http://www.ensembl.org/Mus_musculus/geneview) must have had an influence on the reproductive system of female mutants. A preferential loss of maternally transmitted allele was reported in the CBA/H mouse model of radiation-induced acute myeloid leukemia.[22] The loss of imprinting of the insulin like growth factor II gene triggered acute myeloid leukemia.[23]

The spontaneous development of intestinal tumors in *Pax6*^{Sey3H} was unique. There has been no report in which any of the six known genes in the deleted segment were associated with intestinal tumors. No gene whose mutations developed intestinal tumors spontaneously with a high frequency were located on chromosome 2 (Category of Mouse Tumor Biology, http://tumor.informatics.jax.org).[24-40] Intestinal tumorigenesis was not promoted by radiation, although the age at exposure was unsuitable for the induction of solid tumors. It is conclusive that intestinal tumorigenesis of *Pax6*^{Sey3H} may be ignored in the discussion of myeloid leukemogenesis, which has been tested under the established system.[11]

Higher proportions of the cumulative survival observed in (JF1 × *Pax6*^{Sey3H}) than those in (C3H × *Pax6*^{Sey3H}) are most likely caused by two factors: the advantageous effects of hybrid and the genetic factor from JF1, one of the wild mouse strains. Because we have not yet examined radiation leukemogenesis with the *Pax6*^{Sey3H} mice backcrossed into JF1, we have been unable to evaluate whether these high survival ratios of (JF1 × *Pax6*^{Sey3H}) are intermediate between the values of *Pax6*^{Sey3H} onto C3H/He and those onto JF1.

AKNOWLEDGEMENTS

The authors thank Dr. K. Yamamura for useful discussion and Dr. S. Kitou for recovering mice from frozen embryos. This work was supported by a grant from the Ministry of Education, Culture, Sports, Science and Technology (Tokyo, Japan) (Y.N., 1287092).

REFERENCES

1. Ichimaru, M. and Ishimaru, T. (1975) Leukenia and related disorders. Radiat. Res. Suppl. **16**: 89–96.
2. Kodama, K., Mabuchi, K. and Shigenatsu, I. (1996) A long-term cohot study of the atomic-bomb survivors. J. Epidemiol. **6** (**Suppl.**): 95–105.
3. Pierce, D. A., Shimizu, Y., Preston, D. L., Vaeeth, M. and Mabuchi, K. (1996) Studies of mortality of atomic bomb survivors. Report 12. Part I. Cancer: 1950–1990. Radiat. Res. **146**: 1–27.
4. Nakanishi, M., Tanaka, K., Shintani, T., Takahashi, T. and Kamada, N. (1999) Chromosomal instability in acute myelocytic leukemia and myelodysplastic syndrome patients among atomic bomb survivors. J. Radiat. Res. **40**: 159–167.
5. Hayata, I., Ishihara, T., Hirashima, K., Sado, T. and Yamagiwa, J. (1979) Partial deletion of chromosome 2 in myeloid leukemias of irradiated C3H/He and RFM mice. J. Natl. Cancer Inst. **63**: 843–848.
6. Hayata, I., Seki, M., Yoshida, K., Hirashima, K., Sado, T., Yamagiwa, J. and Ishihara, T. (1983) Chromosomal aberrations observed in 52 mouse myeloid leukemias. Cancer Res. **43**: 367–373.
7. Alexander, B. J., Rasko, J. E. J., Morahan, G. and Cook, W. D. (1995) Gene deletion explains both in vivo and in vitro generated chromosome 2 aberrations associated with murine myeloid leukemia. Leukemia **9**: 2009–2015.
8. Silver, A., Moody, J., Dunford, R., Clark, D., Ganz, S., Bulman, R., Boiuffler, S., Finnon, P., Meijne, E., Kuiskamp, R. and Cox, R. (1999) Molecular mapping of chromosome 2 deletions in murine radiation-induced AML localizes a putative tumor suppressor gene to a 1.0cM region homologous to human chromosome segment 11p11~12. Genes Chromosome Cancer **24**: 95–104.
9. Rithidech, K., Dunn, J. J., Roe, B. A., Gorden, R. and Cronkite, E. P. (2002) Evidence for two commonly deleted regions on mouse chromosome 2 in gamma-ray-induced acute myeloid leukemic cells. Exp. Hematol. **30**: 564–570.
10. Hill, R. E., Favor, J., Hogan, B. L. M., Tom, C. C., Saunders, G. F., Handon, I. M., Prosser, J., Jordan, T., Hastie, N. D. and Van Heyningen, V. (1991) Mouse small eye results from mutations in a paired-like homeobox-containing gene. Nature **354**: 522–525.
11. Seki, M., Yoshida, K., Nishimura, M. and Nemoto, K. (1991) Radiation-induced myeloid leukemia in C3H/HeNirsMs mice and the effect of predonizolone acetate on leukemogenesis. Radiat. Res. **127**: 146–155.
12. Nitta, Y., Yoshida, K., Tanaka, K., Peters, J. and Cattanach, B. M. (2002) The mouse small eye mutant, Del (2)Sey3H which deletes the putative tumor suppressor region of the radiation-induced acute myeloid leukemia is susceptible to radiation. In: Molecular Mechanisms for Radiation-induced Cellular response and Cancer Development, Eds. K. Tanaka, T. Takabatake, K. Fujikawa, T. Matsumoto, and F. Sato, pp. 136–142, Institute of Environment Science Press, Aomori.
13. Nitta, Y. and Hoshi, M. (2003) Relationship between oocyte apoptosis and ovarian tumors induced by high and low LET radiations in mice. Int. J. Radiat. Biol. **79**: 241–250.
14. Robinson, C. V. and Upton, A. C. (1978) Competing-risk analysis of leukemia and nonleukemia mortality in X-irradiatewd, male RF mice. J. Natl. Cancer Inst. **60**: 995–1007.
15. Yosihida, K., Aizawa, S., Watanabe, K., Hirabayashi, Y. and Inoue, T. (2002) Stem-cell leukemia: p53 deficient mediated suppression of leukemic differentiation in C3H/He myeloid leukemia. Leukemia Res. **26**: 1085–1092.
16. Ban, N., Yoshida, K., Aizawa, S., Wada, S. and Kai, M. (2002) Cytogenetic analysis of radiation-induced leukemia in Trp53-deficient C3H/He mice. Radiat. Res. **158**: 69–77.
17. Macdonald, D., Boulton, E., Pocock, D., Goodhead, D.,

Kadhim, M. and Plumb, M. (2001) Evidence of genetic instability in 3Gy X-ray-induced mouse leukemias and 3Gy X-irradiated hematopoietic stem cells. Int. J. Radiat. Biol. **77**: 1023–1031.
18. Dumon-Jones, V., Frappart, P. O., Tong, W. M., Sajithlal, G., Hulla, W., Schmid, G., Herceg, Z., Digweed, M. and Wang, Z. Q. (2003) Nbn heterozygosity renders mice susceptible to tumor formation and ionizing radiation-induced tumorigenesis. Cancer Res. **63**: 7263–7269.
19. Srivastava, M., Montagna, C., Leighton, X., Glasman, M., Naga, S., Eidelman, O., Ried, T. and Pollard, H. B. (2003) Haploinsufficiency of Anx7 tumor suppressor gene and consequent genomic instability promotes tumorigenesis in the Anx7(+/–) mouse. Proc. Natl. Acad. Sci. USA **100**: 14287–14292.
20. Bouffler, S. D., Hofland N., Cox, R. and Fodde, R. (2000) Evidence for Msh2 haploinsufficiency in mice revealed by MNU-induced sister-chromatid exchange analysis. Br. J. Cancer **83**: 1291–1294.
21. Yoshida, K., Nemoto, K., Nishimura, M. and Seki, M. (1993) Exacerbating factors of radiation-induced myeloid leukemogenesis. Leukemia Res. **17**: 437–440.
22. Cleary, H., Boulton, E. and Plumb, M. (2001) Allelic loss on chromosome 4 (Lyr2/TLSR5) is associated with myeloid, B-lympho-myeloid, and lymphoid (B and T) mouse radiation-induced leukemias. Blood **98**: 1549–1554.
23. Houtenbos, I. and Ossenkoppele, G. J. (2002) Acute myeloid leukemia in a 23-year-old patient with Beckwith-Wiedemann syndrome. Cancer Genet Cytogenet. **136**: 90–91.
24. Moser, A. R., Pitot, H. C. and Dove, W. F. (1990) A dominant mutation that predisposes to multiple intestinal neoplasia in the mouse. Science **247**: 322–324.
25. Edelmann, W., Yang, K., Kuraguchi, M., Heyer, J., Lia, M., Kneitz, B., Fan, K., Brown, A. M., Lipkin, M. and Kucherlapati, R. (1999) Tumorigenesis in Mlh1 and Mlh1/Apc1638N mutant mice. Cancer Res. **59**: 1301–1307.
26. Halberg, R. B., Katzung, D. S., Hoff, P. D., Moser, A. R., Cole, C. E., Lubet, R. A., Donehower, L. A., Jacoby, R. F. and Dove, W. F. (2000) Tumorigenesis in the multiple intestinal neoplasia mouse: Redundancy of negative regulators and specificity of modifiers. Proc. Natl. Acad. Sci. USA **97**: 3461–3466.
27. Silverman, K. A., Koratkar, R., Siracusa, L. D. and Buchberg, A. M. (2002) Identification of the Modifier of Min 2 (Mon2) locus, a new mutation that influences Apc-induced intestinal neoplasia. Genome Res. **12**: 88–97.
28. Song, S. Y., Gannon, M., Washington, M. K., Scoggins, C. R., Meszoely, I. M., Goldenring, J. R., Marino, C. R., Sandgren, E. P., Coffey, R. J. Jr, Wright, C. V. and Leach, S. D. (1999) Expansion of Pdx1-expressing pancreatic epithelium and islet neogenesis in transgenic mice overexpressing transforming growth factor alpha. Gastroenterology **117**: 1416–1426.
29. Dudley, M. E., Sundberg, J. P. and Roopenian, D. C., (1996) Frequency and histological appearance of adenomas in multiple intestinal neoplasia mice are unaffected by severe combined immunodeficiency (scid) mutation. Int. J. Cancer **65**: 249–253.
30. Fazeli, A., Steen, R. G., Dickinson, S. L., Bautista, D., Dietrich, W. F., Bronson, R. T., Bresalier, R. S., Lander, E. S., Costa, J. and Weinberg, R. A. (1997) Effects of p53 mutations on apoptosis in mouse intestinal and human colonic adenomas. Proc. Natl. Acad. Sci. USA **94**: 10199–10204.
31. Goss, K. H., Risinger, M. A., Kordich, J. J., Sanz, M. M., Straughen, J. E., Slovek, L. E., Capobianco, A. J., German, J., Boivin, G. P. and Groden, J. (2002) Enhanced tumor formation in mice heterozygous for Blm mutation. Science **297**: 2051–2053.
32. Harada, N., Tamai, Y., Ishikawa, T., Sauer, B., Takaku, K., Oshima, M. and Taketo, M. M. (1999) Intestinal polyposis in mice with a dominant stable mutation of the beta-catenin gene. EMBO J. **18**: 5931–5942.
33. Franklin, D. S., Godfrey, V. L., O'Brien, D. A., Deng, C. and Xiong, Y. (2000) Functional collaboration between different cyclin-dependent kinase inhibitors suppresses tumor growth with distinct tissue specificity. Mol. Cell. Biol. **20**: 6147–6158.
34. Di, Cristofano, A., De, Acetis, M., Koff, A., Cordon-Cardo, C. and Pandolfi, P. P. (2001) Pten and p27KIP1 cooperate in prostate cancer tumor suppression in the mouse. Nat. Genet. **27**: 222–224.
35. Anderson, P., McGuire, J., Rubio, C., Gradin, K, Whitelaw, M. L., Pettersson, S., Hanberg, A. and Poellinger, L. (2002) A constitutively active dioxin/aryl hydrocarbon receptor induces stomach tumors. Proc. Natl. Acad. Sci. USA **99**: 9990–9995.
36. Chawengsaksophak, K., James, R., Hammond, V, E., Kontgen, F. and Beck, F. (1997) Homeosis and intestinal tumours in Cdx2 mutant mice. Nature **386**: 84–87.
37. Takaku, K., Miyoshi, H., Matsunaga, A., Oshima, M., Sasaki, N., Taketo, and M. M. (1999) Gastric and duodenal polyps in Smad4 (Dpc4) knockout mice. Cancer Res. **59**: 6113–6117.
38. Boivin, G. P., Washington, K., Yang, K., Ward, J. M., Pretlow, T. P., Russell, R., Besselsen, D. G., Godfrey, V. L., Doetschman, T., Dove, W. F., Pitot, H. C., Halberg, R. B., Itzkowitz, S. H., Groden, J. and Coffey, R. J. (2003) Pathology of mouse models of intestinal cancer: Consensus report and Recommendations. Gastroenterology **214**: 762–777.
39. Velcich, A., Yang, W., Heyer, J., Fragale, A., Nicholas, C., Viani, S., Kucherlapati, R., Lipkin, M., Yang, K. and Augenlicht, L. (2002) Colorectal cancer in mice genetically deficient in the mucin Muc2. Science **295**: 1726–1729.
40. Li, Q. L., Ito, K., Sakakura, C., Fukamachi, H., Inoue, K., Chi, X. Z., Lee, K. Y., Nomura, S., Lee, C. W., Han, S. B., Kim, H. M., Kim, W. J., Yamamoto, H., Yamashita, N., Yano, T., Ikeda, T., Itohara, S., Inazawa, J., Abe, T., Hagiwara, A., Yamagishi, H., Ooe, A., Kaneda, A., Sugimura, T., Ushijima, T., Bae, S. C. and Ito, Y. (2002) Causal relationship between the loss of RUNX3 expression and gastric cancer. Cell **109**: 113–124.

Received on September 16, 2003
1st Revision on November 4, 2003
2nd Revision on January 5, 2004
3rd Revision on January 27, 2004
Accepted on January 30, 2004